J Neurophysiol 99: 2844–2863, 2008.
First published April 9, 2008; doi:10.1152/jn.00986.2007.

Serotonin Transduction Cascades Mediate Variable Changes in Pyloric Network Cycle Frequency in Response to the Same Modulatory Challenge

Nadja Spitzer,[1] Gennady Cymbalyuk,[2] Hongmei Zhang,[1] Donald H. Edwards,[1] and Deborah J. Baro[1]
[1]*Department of Biology and* [2]*Department of Physics and Astronomy, Georgia State University, Atlanta, Georgia*

Submitted 3 September 2007; accepted in final form 27 March 2008

Spitzer N, Cymbalyuk G, Zhang H, Edwards DH, Baro DJ. Serotonin transduction cascades mediate variable changes in pyloric network cycle frequency in response to the same modulatory challenge. *J Neurophysiol* 99: 2844–2863, 2008. First published April 9, 2008; doi:10.1152/jn.00986.2007. A fundamental question in systems biology addresses the issue of how flexibility is built into modulatory networks such that they can produce context-dependent responses. Here we examine flexibility in the serotonin (5-HT) response system that modulates the cycle frequency (cf) of a rhythmic motor output. We found that depending on the preparation, the same 5-min bath application of 5-HT to the pyloric network of the California spiny lobster, *Panulirus interruptus*, could produce a significant increase, decrease, or no change in steady-state cf relative to baseline. Interestingly, the mean circuit output was not significantly different among preparations prior to 5-HT application. We developed pharmacological tools to examine the preparation-to-preparation variability in the components of the 5-HT response system. We found that the 5-HT response system consisted of at least three separable components: a 5-$HT_{2\beta Pan}$-like component mediated a rapid decrease followed by a sustained increase in cf; a 5-$HT_{1\alpha Pan}$-like component produced a small and usually gradual increase in cf; at least one other component associated with an unknown receptor mediated a sustained decrease in cf. The magnitude of the change in cf produced by each component was highly variable, so that when summed they could produce either a net increase, decrease, or no change in cf depending on the preparation. Overall, our research demonstrates that the balance of opposing components of the 5-HT response system determines the direction and magnitude of 5-HT–induced change in steady-state cf relative to baseline.

INTRODUCTION

Rhythmic motor patterns such as locomotion, respiration, and chewing are essential to the function and survival of an animal. The central pattern generators (CPGs) responsible for producing such rhythmic outputs depend on neuromodulation to maintain their cycle and to appropriately modify their output parameters (Fenelon et al. 2004; Hooper and DiCaprio 2004; Marder and Bucher 2001, 2007; Selverston 2005; Thoby-Brisson and Simmers 1998). It has been shown that the responses of neural circuits to the same neuromodulator can change depending on the experience or physiological state of the animal (Birmingham et al. 2003; Edwards et al. 2002; Mitchell and Johnson 2003; Yeh et al. 1997). This can occur through changes in synaptic strength, intrinsic neuronal properties, cell morphology, and gene expression; however, the signaling cascades leading to these changes, and the way in which these mechanisms are restructured in a behaviorally relevant manner, are not clear (Carlisle and Kennedy 2005; Davis 2006; Kandel 2001; Mitchell and Johnson 2003; Yuan and Chen 2006). The first step in understanding this plasticity in neuromodulatory response systems is to delineate the components of the system and how they vary across preparations in response to the same modulatory input.

The stomatogastric nervous system (STNS) of crustaceans is a well-established model for investigating the circuitry and neuromodulation of motor pattern generation. The STNS contains several small, defined circuits, each of which drives a different set of muscles to produce a patterned activity associated with a specific function. One such circuit, the pyloric network, located in the stomatogastric ganglion (STG), consists of 14 identified neurons that fall into six cell types (Selverston et al. 1976). The intrinsic firing properties and synaptic connectivities of each cell type have been described in detail (Harris-Warrick et al. 1992a; Nusbaum and Beenhakker 2002; Selverston 2005). In addition, the effects of neuromodulators, including serotonin (5-HT), have been investigated at the cellular and circuit levels (Ayali and Harris-Warrick 1999; Beltz et al. 1984; Flamm and Harris-Warrick 1986a,b; Harris-Warrick et al. 1992b, 1998; Katz and Harris-Warrick 1990; Peck et al. 2001).

In the California spiny lobster, *Panulirus interruptus*, 5-HT is not found in STG nerve terminals. Instead, it acts solely as a neurohormone to directly alter the firing properties of several pyloric neurons. A 10-min 5-HT application intended to mimic neurohormonal transmission elicited bursting from the anterior burster (AB) neuron (Ayali and Harris-Warrick 1999; Harris-Warrick and Flamm 1987), inhibited firing in the lateral pyloric (LP) and ventricular dilator (VD) neurons, excited the inferior cardiac (IC) neuron, and had no effect on the pyloric dilator (PD) or pyloric constrictor (PY) neurons (Ayali and Harris-Warrick 1999; Flamm and Harris-Warrick 1986b). In addition, 5-HT modulated the strength of electrotonic coupling and chemical synapses within the circuit (Johnson and Harris-Warrick 1990; Johnson et al. 1993, 1994, 1995). The effects of 5-HT are mediated, at least in part, by cell-specific targeting of ionic currents (Harris-Warrick et al. 1998; Kiehn and Harris-Warrick 1992; Peck et al. 2001; Zhang and Harris-Warrick 1995).

Arthropods are known to express multiple 5-HT receptor (5-HTR) types (Tierney 2001). In all, five arthropod 5-HTR subtypes have been cloned and characterized to date: two 5-HT_1 receptors, two 5-HT_2 receptors, and a 5-HT_7 receptor (Clark et al. 2004; Colas et al. 1995; Saudou et al. 1992; Witz

Address for reprint requests and other correspondence: D. J. Baro, Georgia State University, Department of Biology, P.O. Box 4010, Atlanta, GA 30302-4010 (E-mail: dbaro@gsu.edu).

The costs of publication of this article were defrayed in part by the payment of page charges. The article must therefore be hereby marked "*advertisement*" in accordance with 18 U.S.C. Section 1734 solely to indicate this fact.

et al. 1990). In addition, analysis of arthropod genomic databases suggests the presence of three putative monoamine receptors that currently remain uncharacterized (discussed in Clark and Baro 2007; Clark et al. 2004). The arthropod genome therefore most likely contains from five to eight genes encoding 5-HTRs.

Here we investigate the components of the 5-HT response system that control pyloric cycle frequency (cf) in the California spiny lobster. Application of 5-HT to individual preparations that appeared to be in the same state uncovered latent preparation-to-preparation variability in the network. We found that pyloric networks producing motor outputs with similar cycle frequencies could respond to 5-HT application with either an increase, decrease, or no change in pyloric cf, depending on the preparation. We then identified pharmacological tools to differentiate the actions of the two previously cloned and characterized crustacean receptors, 5-$HT_{2\beta}$ and 5-$HT_{1\alpha}$ (Clark et al. 2004; Sosa et al. 2004; Spitzer et al. 2008). Finally, we used these tools to define the components of the 5-HT response system and determine how each component contributes to the variability in a network's response to the same modulatory input.

METHODS

Animals

Spiny lobsters, *Panulirus interruptus*, were obtained from Don Tomlinson Commercial Fishing (San Diego, CA) and maintained at 16°C in continually filtered and aerated artificial seawater. Animals were fed once per week with raw shrimp. The number of shrimp added to the tank was two to five more than the number of lobsters in the tank, but no attempt was made to ensure that each lobster received food.

Chemicals and cell lines

HEK293 cells, EMEM, horse serum, trypsin, and penicillin/streptomycin were obtained from American Type Culture Collection (Manassas, VA). DMEM was from Mediatech (Herndon, VA). Dialyzed fetal bovine serum (FBS), TRex cell line (293-TR), pDNA4/TO plasmid, blasticidin, and zeocin were from Invitrogen (Carlsbad, CA). Cinanserin was obtained from Tocris (Ballwin, MO). All other chemicals were from Sigma (St. Louis, MO). For pharmacology experiments, fresh amine and agonist stock solutions (10^{-1} M) were made in media or 50% ethanol, respectively. Two exceptions were tyramine, which was made fresh as a 10^{-2} M stock in media, and methysergide, which was made as a 10^{-2} M stock in DMSO and stored at −20°C. Antagonist drugs were made as 10^{-2} M stock solutions in DMSO and stored at −20°C. To test the effect of DMSO on deafferented preparations, we applied 5-HT for 5 min, washed out for 1 h, and applied DMSO for 5 min and then DMSO + 5-HT for 5 min. In the absence of 5-HT, application of DMSO for 5 min did not produce a detectable change in cf ($P > 0.23$, $n = 4$, also see Fig. 5). Neither did DMSO application alter the steady-state 5-HT response. The 5-HT–induced change from baseline (average of last 10 cycles during 5-min 5-HT application/average for last 10 cycles just before 5-HT application) was not significantly different in the absence (0.93 ± 0.21) versus the presence of DMSO (0.96 ± 0.24, $P > 0.71$, $n = 3$).

Electrophysiological recordings

Spiny lobsters were anesthetized for ≥30 min on ice, after which the STNS was dissected out and pinned in a Sylgard-lined petri dish using standard techniques (Selverston et al. 1976). The stomatogastric ganglion (STG) and a portion of the stomatogastric nerve (*stn*) were desheathed. The preparation was bathed in *Panulirus* saline consisting of (in mM) 479 NaCl, 12.8 KCl, 13.7 $CaCl_2$, 39 Na_2SO_4, 10 $MgSO_4$, 2 glucose, 4.99 HEPES, and 5 TES at pH 7.4. All experiments were carried out at room temperature. Petroleum jelly (Vaseline) wells (1–2 cm across) were built around the STG and around the desheathed portion of the *stn*. Both wells were always tested for leaks with saline containing 0.005% Fast Green. The well around the STG was constantly perfused at 2 ml/min with saline or drug solutions and tests with Fast Green prior to every experiment showed that the solution in the STG well was completely exchanged in <20 s.

Extracellular recordings from the pyloric dilator nerve (*pdn*), medial ventricular nerve (*mvn*), and lateral ventricular nerve (*lvn*) were obtained with stainless steel pin electrodes and a differential AC amplifier (A-M Systems, Everett, WA) as previously described (Baro et al. 1997). In some preparations, the activity of the PD neuron was monitored with intracellular somatic recordings using glass microelectrodes filled with 3 M KCl (20–30 MΩ) and an Axoclamp 2B amplifier (Axon Instruments, Foster City, CA). In these cases, the PD was identified by the characteristic shape of its oscillation, by its timing in the motor pattern, and by a 1:1 correlation between action potentials recorded intracellularly from the soma and extracellularly from the *pdn*.

After recording baseline activity for 10 min, the saline solution in the *stn* well was exchanged for 1 M sucrose to block descending neuromodulatory input. After 1 h in the sucrose block, experiments to determine the effects of 5-HT receptor agonists and antagonists were performed. For experiments to determine the effect of the agonist 1-(*m*-chlorophenyl)-piperazine (mCPP), 10 μM 5-HT was applied for 5 min and washed out for 1 h, followed by a 5-min application of 100 μM mCPP, which was then washed out for 1 h. The antagonist (+)butaclamol (10 μM) was then applied for 5 min followed immediately by a 5-min application of (+)butaclamol + mCPP. After another 1-h wash (+)butaclamol was applied for 5 min followed by 5 min of (+)butaclamol + 5-HT. The preparation was washed for a final 1 h and the experiment was terminated. In some experiments, the order of 5-HT and mCPP application was reversed, with no detectable difference in effect. For experiments involving only 5-HT and antagonists [cinanserin or (+)butaclamol], 1 h after applying a sucrose block, 5-HT was applied for 5 min and washed out for 1 h. The antagonist was then applied alone for 5 min and then in combination with 5-HT for 5 min followed by a 1-h wash. After application of one antagonist the experiment was terminated and the preparation was not used further. In several experiments we applied antagonist plus 5-HT before 5-HT only; however, we found that the antagonist effects did not appear to wash out between applications (i.e., both 5-HT applications produced a similar effect, which was not the case when the order was reversed).

Electrophysiological data acquisition and analysis

Data were acquired using a Digidata 1322A data acquisition board (Axon Instruments) and Axoscope software. The data were subsequently analyzed with DataView 4.7a (W. J. Heitler, University of St. Andrews, Scotland), Microsoft Excel, and Matlab (MathWorks, Natick, MA). We measured agonist- and antagonist-induced changes in two parameters: pyloric cf and spikes per burst of the VD (ventricular dilator) neuron. One cycle was defined as the period extending from the first spike in one PD burst to the first spike in the following PD burst. The cf and number of VD spikes per cycle were first plotted as a function of time for each experiment.

Baseline cf was determined from 10 cycles just before application of a drug when the preparation was in a periodic state (i.e., 1 h after the sucrose block was applied or at the end of a 1-h wash period). The time course of the 5-HT effect could be divided into three quantifiable phases. As a measure of phase 1 we obtained the nadir, i.e., lowest cf (averaged for a 10 s window) during the first 50 s in 5-HT. As a

measure of phase 2 we obtained the peak maximal cf (averaged for a 10 s window) from 50 to 120 s of 5-HT application. As a measure of phase 3 (i.e., steady-state) we obtained the average cf during the last minute of 5-HT application.

Difference traces representing the 5-$HT_{2\beta Pan}$-like component of the 5-HT response system were produced by subtracting cf plots obtained in the presence of 5-HT and 5-$HT_{2\beta Pan}$ antagonist from those obtained in the presence of 5-HT and absence of antagonist. A script was written in Matlab to perform this function. The data accessed by the script are termed the *row data*. The result of the analysis is a curve called a *trace average*, with values assigned for 0.05-min time steps. The trace average for a given set of row data was calculated using uniform 0.15-min time intervals and a sliding window that moved in increments of 0.05 min. Examples of these analyses are shown in Fig. 6. Each set of *left* and *right panels* in Fig. 6 represents the analyses for a single preparation. The *left panels* show two trace averages plotted on top of their respective row data. Consider a single *left panel*. The set of blue data points represents the instantaneous cf recorded during a 5-min 5-HT application. These are the data that were processed by the script (i.e., the row data) to generate the trace average, which is shown as a blue line. The row data and trace average for the instantaneous cf obtained in the presence of 5-HT plus antagonist are similarly plotted in green. Now consider the corresponding *right panel*. The gold trace was obtained by subtracting the green trace average from the blue trace average. Therefore the gold difference trace represents the change in cf mediated by activation of 5-$HT_{2\beta Pan}$-like receptors in that preparation. Baselines for the trace averages were arbitrarily set to zero prior to subtraction. Thus at any given point in time, the 5-$HT_{2\beta Pan}$ component is calculated to be: $(f_{\text{5-HT}} - f_{\text{5-HT baseline}}) - (f_{\text{5-HT+antagonist}} - f_{\text{antagonist baseline}})$, where 5-HT baseline and antagonist baselines are defined in Fig. 4 and f = frequency.

Figure 7*A* plots the mean of the 24 trace averages obtained in the presence of 5-HT. Figure 7*B* shows the mean of the 24 trace averages obtained in 5-HT + antagonist. The mean of the 24 difference traces is shown in Fig. 7*C*.

Statistical analyses were performed with Excel (Microsoft) and Prism (GraphPad) as indicated. The three-dimensional (3-D) plots were generated with Sigmaplot (Systat). Unless otherwise indicated, means are followed by SE, and significance was judged to be $P < 0.05$.

Assay of IP release in cells expressing 5-$HT_{2\beta Pan}$

5-$HT_{2\beta Pan}$ was transiently expressed in HEK293 cell culture, and inositol phosphate (IP) release in cells expressing 5-$HT_{2\beta Pan}$ was assayed using previously described protocols (Clark et al. 2004; Spitzer et al. 2008). Briefly, transiently transfected cells expressing 5-$HT_{2\beta Pan}$ were split into wells on a 24-well plate with 1 μCi/ml of ^{3}H-myoinositol (Amersham, Piscataway, NJ) and allowed to grow to 95–100% confluency over 48 h. The cells were washed with fresh EMEM and then exposed to 10 mM LiCl in EMEM for 20 min at 37°C. As applicable, antagonists were added to individual wells and allowed to incubate for an additional 10 min. 5-HT or agonist drugs were added to test wells and cells were returned to 37°C for 60 min. The medium was removed and replaced with ice-cold 20 mM formic acid. Plates were then placed on ice for 30 min. The cell lysate was collected and applied to AG1-X8 columns (BioRad, Hercules, CA) equilibrated with 20 mM formic acid. The columns were washed with 50 mM ammonium hydroxide followed by elution of IP with 10 ml of 1 M ammonium formate/0.1 M formic acid. The IP fraction was scintillation counted. Membranes attached to the wells were dissolved in 1 M NaOH and scintillation counted as total phosphatidyl inositols (PIs). Activation results are expressed as the fraction of radioactivity incorporated in IP over that in IP + PI and normalized to activity observed in negative control (no drug) wells for every experiment. At least three independent experiments were performed for each drug.

cAMP concentration determinations in cells expressing 5-$HT_{1\alpha Pan}$

5-$HT_{1\alpha Pan}$ was stably expressed in an inducible expression system and cyclic AMP levels were determined using a Direct cAMP kit (Assay Designs, Ann Arbor, MI) as previously described (Spitzer et al. 2008). Briefly, stably transfected cells were plated in 24-well plates and allowed to grow to 100% confluency. The medium was replaced with 1 ml of complete medium containing 1 μg/ml tetracycline to induce expression of receptor protein. After 18–20 h the medium was replaced with 1 ml of fresh DMEM containing 2.5 mM 3-isobutyl-1-methylxanthine to block phosphodiesterase activity and plates were incubated for 10 min. Antagonists were added to individual wells (if applicable) and allowed to incubate for an additional 10 min. 5-HT or agonists and forskolin (250 nM), a nonspecific activator of adenylyl cyclase, were then added to individual wells and left at 37°C for 30 min. The medium was removed and replaced with 0.5 ml of 0.1 M HCl containing 0.8% Triton X-100. Plates were shaken 30 min at room temperature, the lysate was collected and centrifuged 5 min at 600 *g*, and the supernatant was assayed for cAMP concentration using the Direct cAMP kit and protein concentration using a BCA Protein Assay Kit (Pierce, Rockford, IL). Data are presented as picomoles of cAMP per milligram of protein. At least three independent experiments were performed for each drug.

Heterologous expression system data analysis

Data for all pharmacology assays involving the heterologous expression systems were plotted and analyzed in GraphPad Prism v.4. Dose–response curves were fitted with a standard slope top–bottom or bottom–top dose–response curve to calculate EC/IC_{50} and efficacy values. Unless otherwise indicated, means are followed by the SE.

RESULTS

5-HT application produced a stereotypic inhibition of VD but a variable change in cf

We began this study by establishing the variable actions of 5-HT on pyloric cf. The pyloric circuit in the STNS of *Panulirus* consists of six cell types interconnected by electrical and inhibitory chemical synapses (Fig. 1*A*). The circuit is driven by a pacemaker ensemble consisting of a single AB pacemaker interneuron that is electrically coupled to two PD motoneurons. In addition, two follower motoneurons, VD (one per ganglion) and LP (one per ganglion), feed back onto the pacemaker kernel and play an important role in governing cf (Weaver and Hooper 2003). Endogenous oscillations in the AB neuron and consequent activity of coupled and follower neurons give rise to an identifiable motor output that can be measured extracellularly on efferent motor nerves. We monitored the AB–PD pacemaker kernel with extracellular recordings from the *pdn*, a motor nerve that exclusively contains the two axons of the two PD neurons. VD was monitored with extracellular electrodes on the *mvn*, a motor nerve that exclusively contains the axons of the single VD and IC neurons (Fig. 1*B*, *top*). Although the LP is also important in governing cf (Ayali and Harris-Warrick 1999; Beltz et al. 1984; Mamiya and Nadim 2004; Miller and Selverston 1982; Weaver and Hooper 2003), and is directly inhibited by 5-HT (Flamm and Harris-Warrick 1986b), LP was silent under our experimental conditions (see following text) and not monitored in these studies.

Descending modulatory input can be blocked by placing a pool of sucrose on the single modulatory input nerve (stomatogastric nerve, *stn*). After an hour of sucrose block the pyloric

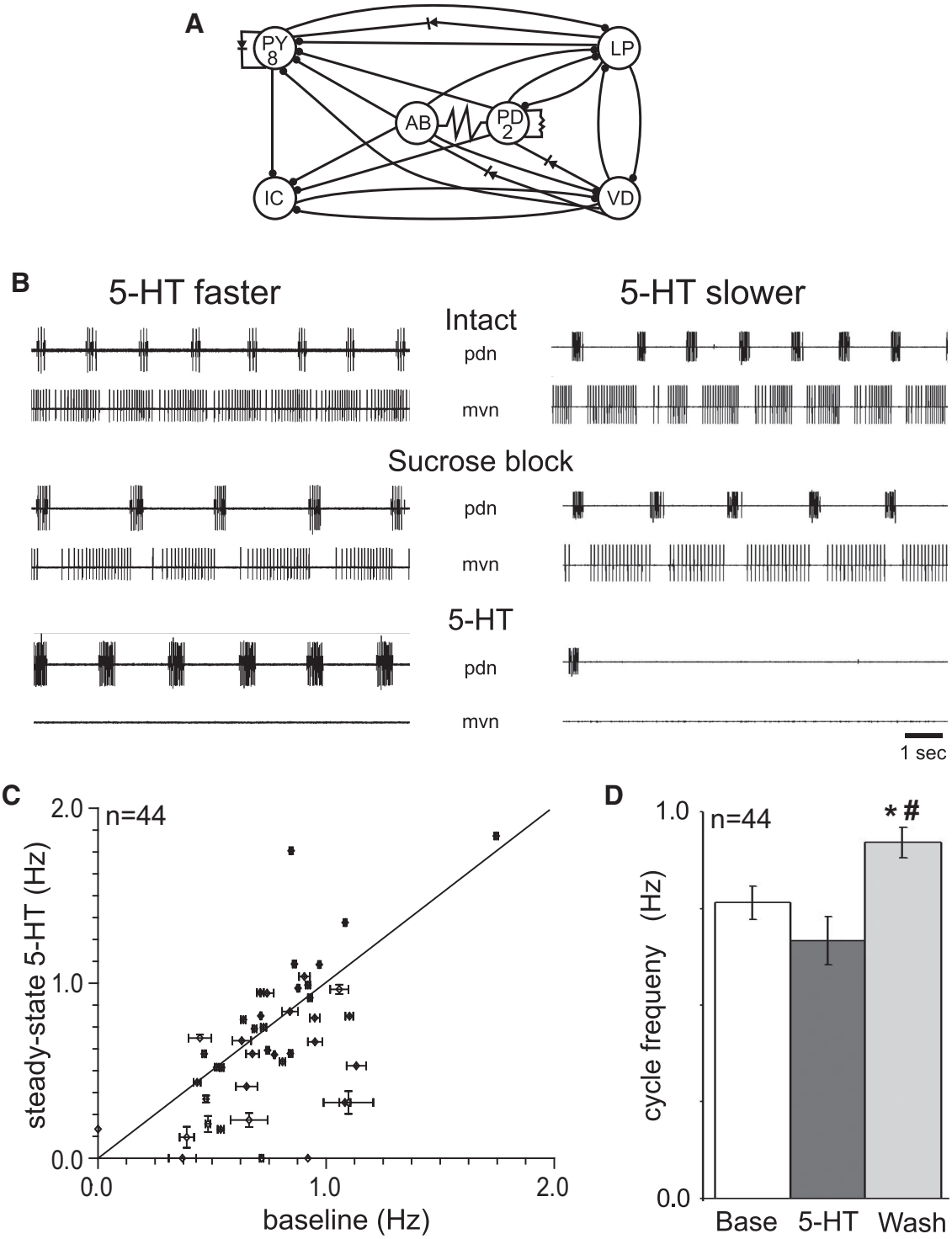

FIG. 1. The pyloric rhythm of the stomatogastric nervous system in spiny lobster is differentially modulated by serotonin (5-HT). *A*: schematic of the pyloric circuit in *P. interruptus* (based on Ayali and Harris-Warrick 1999). Large unfilled circles represent the 6 pyloric cell types. The number of cells in each cell type is indicated, where lack of a number indicates a unique neuron. Small filled circles represent inhibitory chemical synapses. Diodes and resistors represent electrical coupling. *B*: sequential recordings from 2 preparations before sucrose block (*top*), 1 h after sucrose block (*middle*), and in 10^{-5} M 5-HT (*bottom*). Cycle frequency was either increased (*left*) or decreased by 5-HT (*right*). For each set of traces, top extracellular recordings were from the *pdn*, which contains only the 2 pyloric dilator (PD) axons. Thus these traces represent PD activity. Bottom extracellular recordings were from the *mvn*, which contains the axons of the single inferior cardiac (IC) and the single ventricular dilator (VD) neurons. The IC neuron was silent during these recordings; thus these traces represent VD spiking. *C*: the effect of 5-HT on pyloric cycle frequency varies with the preparation. The steady-state 5-HT cycle frequency (average for the last 10 cycles during a 5-min 5-HT application) is plotted against the baseline cycle frequency (average from the last 10 cycles during a 1-h sucrose block, just before 5-HT application) for each of 44 preparations. *x* and *y* error bars represent the SE. Note that 5-HT usually makes preparations more rhythmic such that the *y* error bars are significantly smaller than the *x* ($P < 0.002$, paired *t*-test on the 2 sets of SEs). *D*: on average, 5-HT has no significant effect on pyloric cycle frequency. The bar graphs represent the average baseline and state-state 5-HT response for all 44 preparations plotted in *C*. Additionally, the average cycle frequency after a 10-min washout of 5-HT is shown (average for the last 10 cycles during a 10-min wash). Error bars represent the SE. A repeated-measures ANOVA was performed followed by a Tukey post hoc test: *, significantly different from baseline ($P < 0.05$); #, significantly different from steady-state 5-HT ($P < 0.05$).

cycle stabilizes in a basal cycling state; the pacemaker kernel cycles weakly (Fig. 1*B*, *middle*); VD firing is reduced (Fig. 1*B*, *middle*); and LP, PY (8 per ganglion), and IC neurons are silenced (not shown). Once endogenous neuromodulation is removed with the sucrose block (deafferented preparation), the effect of individual modulators such as 5-HT can be assessed. We used a 5-min application of 5-HT to mimic neurohormonal transmission. This relatively short application was chosen to minimize the induction of long-term effects, but still produce a steady-state response. The concentration of 5-HT used in these studies (10 μM) is likely to be several orders of magnitude higher than the normal hormonal concentration. Thus the actions of neurohormonal 5-HT in vivo may not be exactly reproduced in this study. Nevertheless, the use of this high concentration is appropriate here because the goal of this study was to investigate the latent variability in a network's response to the same modulatory input.

Consistent with previous reports, we found that 5-HT altered the activity of both the pacemaker kernel and the VD neuron. Figure 1*B* shows serial recordings of *pdn* and *mvn* activity from two representative preparations before sucrose block (*top*), 1 h after sucrose block (*middle*), and at the peak of the 5-HT effect (*bottom*). As expected, there was a sustained reduction in VD firing frequency throughout the 5-min 5-HT application. The VD was inhibited by 100% from baseline in 27 of 28 experiments, and the remaining preparation showed a 95% decrease in firing frequency. On the other hand, a 5-min application of 10 μM 5-HT did not produce consistent alterations in cf. 5-HT could increase (Fig. 1*B*, *left pdn traces*), decrease (Fig. 1*B*, *right pdn traces*), or produce no change (not shown) in cf relative to baseline, where baseline was measured after the 1-h sucrose block, immediately before 10 μM 5-HT application.

Figure 1*C* emphasizes the variability in 5-HT effects on cf. The average cf for the last 10 cycles in 5-HT (i.e., steady state 5-HT) was plotted against the average for the last 10 cycles just prior to the addition of 5-HT (i.e., baseline) for every deafferented preparation examined ($n = 44$). Each datum represents a single preparation and the SE. The diagonal line represents unity. Experiments in which 5-HT had no effect fall along the line; those where 5-HT–induced increases or decreases in cf are represented by data points above or below the line, respectively. The average steady-state 5-HT effect for all 44 preparations is plotted in Fig. 1*D*. The representation of the data in this manner is deceptive because it suggests that 5-HT had no significant effect on pyloric cf, which is clearly not the case (Fig. 1*C*).

The variable change in cf did not correlate with gender, molt stage, time/date, or the presence/absence of a spermatophore. It was previously suggested that 5-HT could elicit an increase in cf when the LP was silent and a decrease when the LP cell was active (Beltz et al. 1984). However, this did not seem to be the case in our hands. We obtained extracellular LP recordings from the *lvn* in 20 preparations. After descending modulatory input was removed with a sucrose block, the LP was silent in 17 preparations and fired very weakly and irregularly in the remaining 3. Moreover, it was postulated that the cf decrease was due to LP inhibition of PD. Using 10^{-6} M picrotoxin to suppress glutamatergic transmission (Bidaut 1980), and hence the LP to PD synapse, we still observed an increase or decrease in cf ($n = 3$, data not shown).

Interestingly, washout of 5-HT for 10 min produced a significant increase in cf (Fig. 1*D*). To determine whether the washout effect varied with regard to the 5-HT response, we first classified preparations according to their response. Preparations showing >5% decrease in steady-state 5-HT cf relative to baseline were called Class S for slower. These preparations showed a mean 48 ± 7% decrease in cf over baseline (paired *t*-test, $P < 10^{-5}$, $n = 21$), with individual decreases ranging from about 12 to 100%. Preparations falling into Class F, for faster, showed a mean 26 ± 6% increase in steady-state 5-HT cf from baseline (paired *t*-test, $P = 0.001$, $n = 17$), and individual increases ranged from about 6 to 107%. Preparations displaying <5% change were classified as NC, for no change. These preparations showed a mean 0.0 ± 1.0% decrease in cf over baseline (paired *t*-test, $P > 0.71$, $n = 6$), and changes ranged from a 4% decrease to a 3% increase. The 5-HT effect washed out immediately and completely for all Class S preparations, and then the effect reversed so that by 1 h of wash the cf (average for last 10 cycles of 1-h wash) had significantly increased by an average of 26 ± 15% over the original baseline (Fig. 2*A*). Similarly, all Class F (Fig. 2*B*) and NC (Fig. 2*C*) preparations showed a significant increase over baseline by a 1-h wash. Thus it appeared that the long-term washout effect was the same for all Classes of preparations regardless of their response to 5-HT.

To assess whether the increased baseline was evoked by 5-HT washout or experimental "drift," we recorded for the same length of time from six deafferented preparations that never received 5-HT. Plots of instantaneous cycle frequency versus time showed that in the absence of 5-HT there was a slow steady increase in cf over the course of 70 min (Fig. 3*A*).

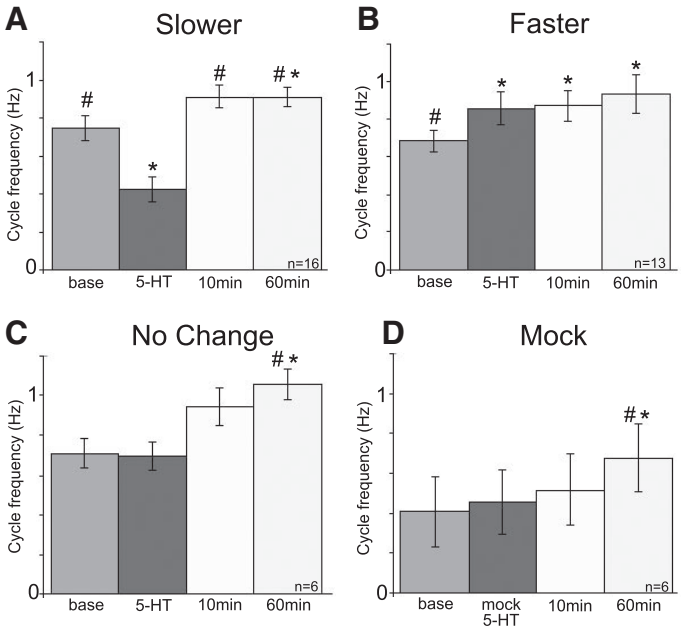

FIG. 2. The increase in cycle frequency observed during 10 μM 5-HT washout is at least partially due to 5-HT–independent phenomena. Preparations were classified on the basis of whether the steady-state 5-HT cycle frequency was slower (*A*), faster (*B*), or unchanged (*C*) relative to baseline as indicated in the text. For each Class, the average cycle frequency for baseline, steady-state 5-HT, and 10- and 60-min washes are plotted. *D*: the same measurements for experiments in which 5-HT was omitted, but that were otherwise identical to those represented in *A–C* (i.e., mock experiments). Error bars, SE; a repeated-measures ANOVA was performed on each of the 4 data sets (*A–D*) followed by a Tukey post hoc test: *, significantly different from baseline ($P < 0.05$); #, significantly different from steady-state 5-HT or steady-state mock 5-HT ($P < 0.05$).

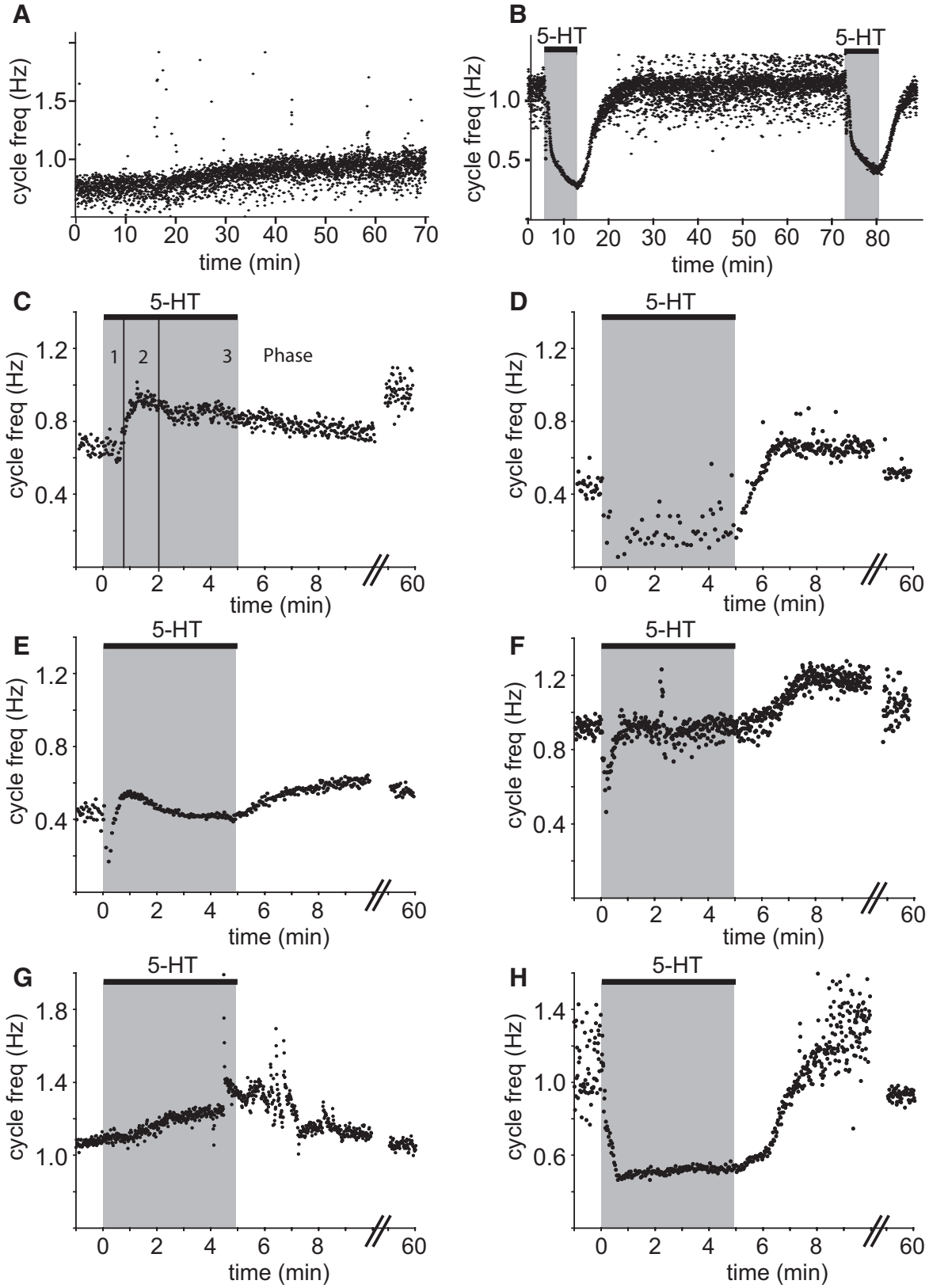

FIG. 3. The time course of the 5-HT response. *A*: pyloric cycle frequency slowly increases over the course of 70 min in the absence of modulatory input. Plot of cycle frequency vs. time for a representative mock experiment ($n = 6$). Each point marks a single pyloric burst. These experiments are exactly like the experiments shown in *C–H*, except that 5-HT was omitted. *B*: sequential applications of 5-HT produce similar effects. Representative plot of cycle frequency vs. time for experiments in which a second 5-HT application followed the 1-h wash ($n = 8$). The gray boxes indicate the times of 5-HT application. *C–H*: the time course of the 5-HT response is variable and complex. In 37 experiments a sucrose block was placed on the *stn* for 1 h; 10 μM 5-HT was next applied for 5 min and then washed out for 1 h. Plots of cycle frequency vs. time for 6 representative experiments are shown before, during, and after 5-HT application. One minute of cycles after the 1-h wash is shown after the hash marks in each plot. The vertical lines in *C* approximate the 3 temporal phases of the response described in the text.

The average of the last 10 cycles during the 1-h sucrose block represented baseline. Figure 2*D* illustrates that there was no significant increase in cf over baseline by 5 min (i.e., the time corresponding to 5 min in 5-HT); however, there was a significant increase over baseline at the time corresponding to the 1-h wash. These data suggest that 5-HT–independent phenomena (e.g., lack of modulatory inputs) could at least partially underpin the changing baseline over the course of the experiment.

We were interested in whether the change in baseline cf over 1 h would alter a deafferented preparation's response to 5-HT. In several experiments ($n = 8$) we applied 5-HT sequentially to a deafferented preparation: 5-HT was applied for 5 min, washed out for 1 h, and then reapplied for 5 min (Fig. 3*B*). We observed that the average responses to the first and second applications of 5-HT were not significantly different (average steady-state 5-HT/baseline = 0.58 ± 0.15 Hz, first application vs. 0.54 ± 0.14 Hz, second application; paired *t*-test, $P = 0.17$, $n = 8$); however, the second response was usually set atop a higher baseline. Importantly, these experiments make the point that 5-HT receptors respond in a like manner to serial 5-min applications of 5-HT spaced at 1-h intervals (see following text).

Three temporal phases of the 5-HT–induced changes in cf

We next examined the time course of the 5-HT–induced changes in cf by plotting the frequency of each pyloric cycle before, during, and after 5-HT application ($n = 37$). Six representative examples are shown in Fig. 3, *C–H*. In about 75% of the experiments (Fig. 2, *C–F*) the time course could generally be described as having three phases: an immediate decrease within the first 50 s of 5-HT application (Phase 1), followed by a slow increase over the next 70 s (Phase 2), which ended in an apparent steady state (Phase 3). The time course and absolute value of the peak within each phase varied according to the preparation. Once peak cf was reached in phase 2, it was either maintained or gradually reached a new apparent steady state (e.g., Fig. 3, *E* vs. *F*). Cycle frequencies were fairly stable after 3 min in 5-HT; however, steady-state 5-HT effects varied greatly, such that the three aforementioned classes of responses were observed (Fig. 3*C*, Class F; Fig. 3*D*, Class S; Fig. 3, *E* and *F*, Class NC). The remaining 25% of the experiments were atypical with regard to time course. These preparations either exhibited no significant response to 5-HT (not shown; Class NC); displayed a small, gradual, significant increase over baseline throughout 5-HT application (Fig. 3*G*, Class F); or showed a fairly dramatic, significant decrease relative to baseline, followed by an apparent steady state (Fig. 3*H*, Class S).

Function and pharmacology of 5-HT$_{2\beta Pan}$

We next sought pharmacological tools that would allow us to characterize the roles of the two previously cloned *Panulirus* 5-HT receptors in generating the 5-HT response. The *Panulirus* 5-HT$_{2\beta Pan}$ receptor has been shown to respond specifically to 5-HT and to couple to the inositol phosphate (IP) signaling pathway when stably expressed in HEK cells (Clark et al. 2004). In this study we transiently expressed 5-HT$_{2\beta Pan}$ in HEK cells and measured IP release in response to amines and putative pharmacological agents. Nontransfected parental HEK cells did not respond to 5-HT in the IP assay. IP levels showed a dose-dependent increase in response to 5-HT in cells expressing 5-HT$_{2\beta Pan}$ with an EC_{50} of 52 nM (Fig. 4*A*, Table 1).

To determine a pharmacological profile for 5-HT$_{2\beta Pan}$ we tested a suite of putative agonist and antagonist drugs. In an initial overview, all drugs were tested at 10^{-3} M (agonists) or 10^{-5} M (antagonists). Agonists that produced a significant increase in IP levels in transfected but not parental lines and antagonists that inhibited the 5-HT–induced increase but had no effect on the parental lines were then used to generate dose–response curves. Typical dose–response curves for agonists and antagonists are shown in Fig. 4*A*. From these curves we determined the potency and efficacy of each drug. The EC_{50} or IC_{50} are measures of the potency of a drug and reflect its binding affinity at the receptor. Because the maximum effect,

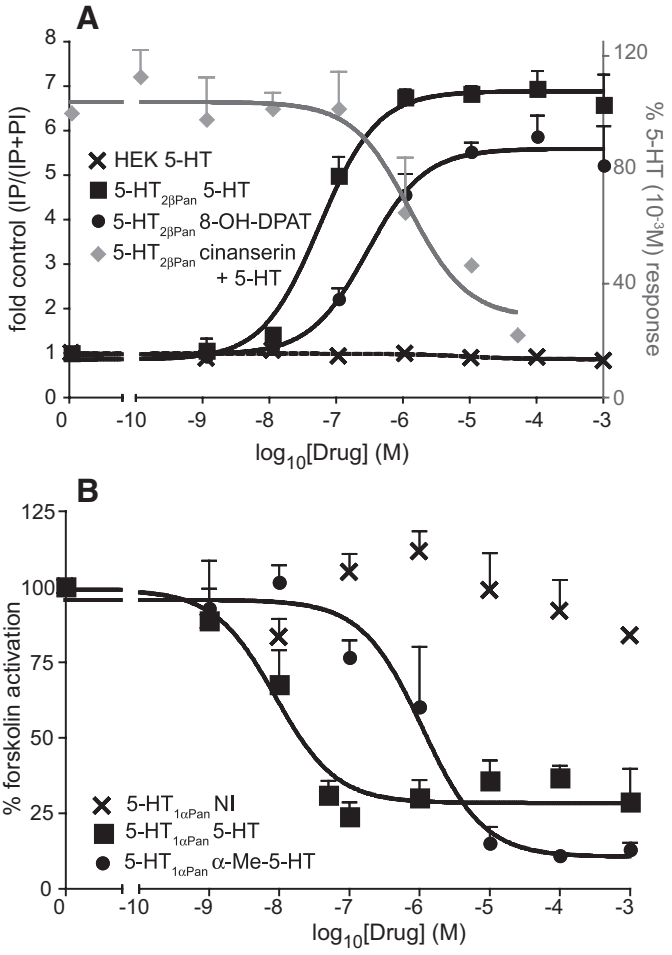

FIG. 4. Signaling and pharmacology of 5-HT$_{2\beta Pan}$ and 5-HT$_{1\alpha Pan}$. *A*: dose–response curves of inositol phosphate (IP) activation in HEK cells. Nontransfected cells do not respond to 5-HT (crosses). Cells expressing 5-HT$_{2\beta Pan}$ respond to 5-HT and an agonist, 8-OH-DPAT, with EC_{50} values of 52 and 270 nM, respectively (black squares and circles). An antagonist, cinanserin, blocks 5-HT activation of 5-HT$_{2\beta Pan}$ with an IC_{50} of 140 nM (gray diamonds). *B*: dose–response curves of cAMP accumulation in 293-TR-5-HT$_{1\alpha Pan}$ cells. In cells induced to express 5-HT$_{1\alpha Pan}$, forskolin-induced accumulation of cAMP is inhibited in response to 5-HT and an agonist, α-Me-5-HT, with EC_{50} values of 8.4 nM and 1.1 μM, respectively (black squares and circles). Noninduced cells did not respond significantly to 5-HT (crosses). Mean ± SE, $n \geq 3$.

TABLE 1. *Agonist profiles of 5-HT$_{2\beta}$ and 5-HT$_{1\alpha}$ from Panulirus*

Drug	Potency (EC_{50}, μM)		Efficacy (% 5-HT Activation)	
	5-HT$_{2\beta Pan}$	5-HT$_{1\alpha Pan}$	5-HT$_{2\beta Pan}$	5-HT$_{1\alpha Pan}$
5-HT	0.052	0.0084	100	100
Dopamine	310	IA	54	IA
Octopamine	IA	IA	IA	IA
Tyramine	283	IA	32	IA
Histamine	IA	IA	IA	IA
DOI	4.5	Bkd	32	Bkd
5-CT	6.1	2.2	79	100
2-Me-5-HT	0.78	Bkd	96	Bkd
MeOTryp	1.0	4.2	80	94
N-Acetyl-5-HT	IA	IA	IA	IA
Quipazine	IA	Bkd	IA	Bkd
α-Me-HT	1.5	1.1	79	120
8-OH-DPAT	0.27	7.6	77	105
mCPP	**IA**	**139**	**IA**	**97**
Methysergide	0.11	0.089	48	81

5-HT$_{2\beta Pan}$ and 5-HT$_{1\alpha Pan}$ were expressed in cultured HEK cells and tested for second-messenger responses to various pharmacological agents. EC_{50} values (potencies) and relative efficacies were calculated from dose–response curves for each drug. Efficacy is presented as a given drug's ability to activate the receptor compared to the maximum activation obtained from 5-HT (100%). Drugs with differential actions on 5-HT$_{2\beta Pan}$ and 5-HT$_{1\alpha Pan}$ are shown in bold. $n \geq 3$ repeated experiments for each drug. IA, drug is inactive; Bkd, drug has background activity on the control noninduced or parental cells and was not tested; DOI, 2,5-dimethoxy-4-iodoamphetamine; 5-CT, 5-carboxamidotryptamine; 2-Me-5-HT, 2-methyl-serotonin; MeOTryp, 5-methoxytryptamine; α-Me-5-HT, α-methyl-serotonin; 8-OH-DPAT, (±)-8-hydroxy-2-(di-*n*-dipropylamino) tetralin; mCPP, 1-(*m*-chlorophenyl)-piperazine.

or efficacy, achieved by any drug is dependent on the number of receptors expressed, we ran a parallel dose–response curve for 5-HT in every experiment and normalized all drug efficacies to the maximum 5-HT response, set at 100%. These data are summarized in Tables 1 and 2.

The following agonist potency rank profile was determined for 5-HT$_{2\beta Pan}$: 5-HT > methysergide > 8-OH-DPAT > 2-Me-5-HT > MeOTryp > α-Me-5-HT > DOI > 5-CT. Although most agonists achieved >75% of 5-HT activation levels, methysergide and DOI were only partial agonists of 5-HT$_{2\beta Pan}$ with efficacies of <50% of the 5-HT effect. No change in IP level was detected after application of 10^{-3} M *N*-acetyl-5-HT, quipazine, or mCPP. None of the drugs had significant effects on nontransfected parental HEK cells.

The rank potency of effective antagonists at 5-HT$_{2\beta Pan}$ was (+)butaclamol > ritanserin > methiothepin > cinanserin > clozapine. Ritanserin and (+)butaclamol, however, were only partially effective in inhibiting activation of 5-HT$_{2\beta Pan}$ by 5-HT even at the highest antagonist concentration. Of the antagonists tested, ketanserin, spiperone, prazosin, (−)butaclamol, gramine, and atropine had no effect at 10^{-5} M. Putative antagonists had no effect on nontransfected parental HEK cells.

Function and pharmacology of 5-HT$_{1\alpha Pan}$

We have functionally characterized crustacean 5-HT$_{1\alpha Pan}$ receptors using a heterologous expression system and demonstrated that these receptors negatively couple with cAMP (Spitzer et al. 2008). In this expression system the 5-HT$_{1\alpha Pan}$ gene is stably integrated into the genome of 293-TR-5-HT$_{1\alpha Pan}$ cells, but the cells do not express the receptor until they are chemically induced to do so. Thus the negative control for this assay is not parental cells, but rather, noninduced 293-TR-5-HT$_{1\alpha Pan}$ cells.

We tested the same suite of potential agonists as before on induced and noninduced 293-TR-5-HT$_{1\alpha Pan}$ cells. Figure 4*B* shows the effect of increasing concentrations of 5-HT$_{1\alpha Pan}$ agonists on cAMP levels in 293-TR-5-HT$_{1\alpha Pan}$ cells that were or were not induced to express 5-HT$_{1\alpha Pan}$ 18–20 h prior to performing the cAMP assay. Although their potencies (EC_{50}) and efficacies (% 5-HT effect) were different, both 5-HT and mCPP elicited a dose-dependent inhibition of forskolin-stimulated cAMP accumulation in induced, but not noninduced, cells. Some agonists (DOI, 2-Me-5-HT, quipazine) had significant effects on noninduced 293-TR-5-HT$_{1\alpha Pan}$ cells and could therefore not be tested on induced cells (indicated as Bkd in Table 1). For each of the remaining drugs, the EC_{50} and the relative efficacy were calculated from dose–response curves similar to those shown in Fig. 4*B*. In this way we generated an agonist profile for the receptor that is summarized in Table 1. The relative potencies of functional agonists at 5-HT$_{1\alpha Pan}$ were: 5-HT > methysergide > α-Me-5-HT > 5-CT > MeOTryp >

TABLE 2. *Antagonist profiles of 5-HT$_{2\beta}$ and 5-HT$_{1\alpha}$ from Panulirus*

Drug	Potency (IC_{50}, μM)		Efficacy (% Reduction)
	5-HT$_{2\beta Pan}$	5-HT$_{1\alpha Pan}$	5-HT$_{2\beta Pan}$
Clozapine	6.8	Bkd	79
Ritanserin	**0.57**	**IA**	**58**
Methiothepin	0.66	Bkd	84
(+)Butaclamol	**0.14**	**IA**	**48**
Cinanserin	**1.2**	**IA**	73
Gramine	IA	IA	IA
(−)Butaclamol	IA	IA	IA
Ketanserin	IA	IA	IA
Spiperone	IA	IA	IA
Prazosin	IA	IA	IA
Atropine	IA	IA	IA
Chlorpromazine	ND	IA	ND
Flupenthixol	ND	IA	ND
Domperidone	ND	IA	ND
Fluphenazine	ND	IA	ND
Haloperidol	ND	IA	ND
Metoclopride	ND	IA	ND
(−)Sulpiride	ND	IA	ND
WAY100635	ND	IA	ND
Yohimbine	ND	IA	ND
S(−)Propanolol	ND	Bkd	ND
SB269970	ND	IA	ND
Metergoline	ND	Bkd	ND
Cyproheptadine	ND	Bkd	ND
SB224289	ND	IA	ND
BRL15572	ND	IA	ND
TFMPP	ND	IA	ND
SCH23390	ND	Bkd	ND
S(−)Eticlopride	ND	Bkd	ND

5-HT$_{2\beta Pan}$ and 5-HT$_{1\alpha Pan}$ were expressed in cultured HEK cells and tested for second-messenger responses to various pharmacological agents. IC_{50} values (potencies) and relative efficacies were calculated from dose–response curves for each drug. Efficacy is presented as the percentage reduction of the total effect obtained from 5-HT in the absence of antagonist. Drugs with differential actions on 5-HT$_{2\beta Pan}$ and 5-HT$_{1\alpha Pan}$ are shown in bold. $n \geq 3$ repeated experiments for each drug. IA, inactive; Bkd, drug has background activity on noninduced or parental cells and was not tested; ND, not determined.

8-OH-DPAT > mCPP. 5-$HT_{1\alpha Pan}$ did not respond significantly to 10^{-3} M *N*-acetyl-5-HT.

We also tested antagonists for their ability to inhibit 5-$HT_{1\alpha Pan}$ activation by 5-HT (Table 2). The antagonist (10^{-5} M) was applied 10 min prior to 5-HT and forskolin-stimulated cAMP levels were determined. Twenty-nine drugs were tested (the suite tested on 5-$HT_{2\beta Pan}$ and 18 additional drugs). Seven antagonists [clozapine, methiothepin, S(−)propanolol, metergoline, cyproheptadine, SCH23390, S(−)eticlopride] had significant effects on noninduced 5-$HT_{1\alpha Pan}$ cells and could therefore not be tested for activity on induced 5-$HT_{1\alpha Pan}$ cells (indicated as Bkd in Table 1). None of the remaining 22 drugs was able to significantly block the inhibition of cAMP accumulation resulting from 5-HT activation of 5-$HT_{1\alpha Pan}$, even when low levels (5×10^{-8} M) of 5-HT were used.

Identification of drugs to differentiate 5-$HT_{2\beta Pan}$ and 5-$HT_{1\alpha Pan}$

Several drugs whose action could differentiate between 5-$HT_{2\beta Pan}$ and 5-$HT_{1\alpha Pan}$ were identified (Tables 1 and 2). The agonist mCPP activates 5-$HT_{1\alpha Pan}$ but not 5-$HT_{2\beta Pan}$. Several 5-$HT_{2\beta Pan}$ antagonists that did not block 5-$HT_{1\alpha Pan}$ receptors were also identified: (+)butaclamol, cinanserin, and ritanserin. We next used these drugs on the native system to study the role of the 5-$HT_{2\beta Pan}$ and 5-$HT_{1\alpha Pan}$ receptors in modulating pyloric cf.

Blocking the 5-$HT_{2\beta Pan}$ transduction cascade significantly alters temporal phases 2 and 3 of the 5-HT response

Figures 1–3 illustrate that the 5-HT–induced change in cf could be divided into three temporal phases (Ph1, Ph2, Ph3) and could vary with the preparation (e.g., Classes F, S, and NC). The mechanisms underlying this temporal progression and preparation-to-preparation variability were unknown. We next set out to determine whether 5-$HT_{1\alpha Pan}$ and 5-$HT_{2\beta Pan}$ receptors were components of the 5-HT response system that controlled cf and, if so, how these components varied with time and across preparations.

We first examined the contribution of 5-$HT_{2\beta Pan}$ receptors to 5-HT modulation of cf. The antagonists (+)butaclamol and cinanserin block 5-HT activation of 5-$HT_{2\beta Pan}$ but not 5-$HT_{1\alpha Pan}$ receptors (Table 2); therefore we applied cinanserin or (+)butaclamol with 5-HT (Fig. 5). Unfortunately, cinanserin and (+)butaclamol could not be used on the same preparation because their antagonistic effects did not wash out. This also prevented us from reversing the order of application

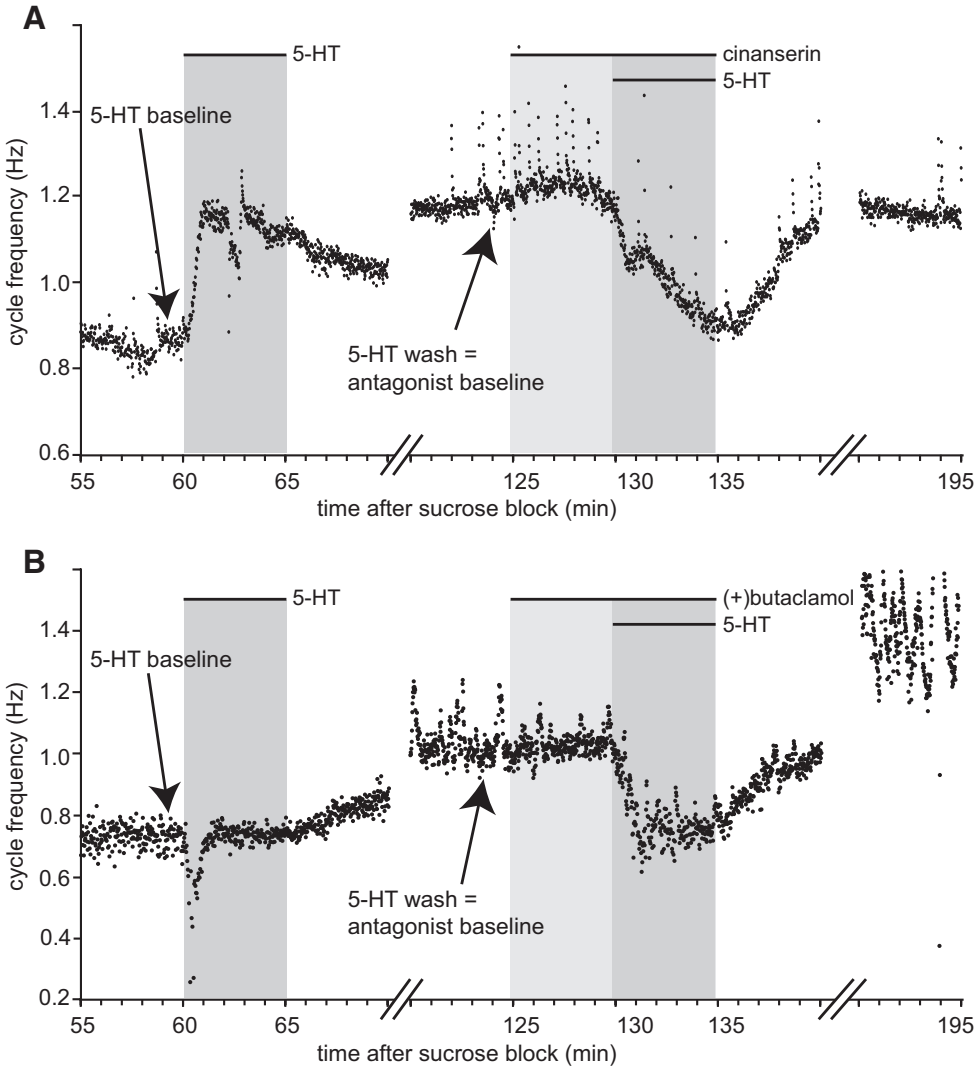

FIG. 5. 5-$HT_{2\beta Pan}$-like receptors contribute to the 5-HT response. Time-course plots of representative experiments showing pyloric cycle frequency during serial application of 10 μM 5-HT alone and with 10 μM cinanserin, $n = 8$ (*A*) or 10 μM (+)butaclamol, $n = 22$ (*B*).

(i.e., we could not perform 5-HT plus antagonist followed by 5-HT alone). Nevertheless, it was clear from qualitative observations (e.g., compare Fig. 5, *A* vs. *B*) and quantitative measurements (see following text) that these drugs produced comparable results. Additionally, preliminary experiments using the 5-$HT_{2\beta Pan}$ antagonist ritanserin (Table 2) yielded similar findings (not shown). The fact that multiple 5-$HT_{2\beta Pan}$ antagonists have the same effect increases the likelihood that these experiments are reporting on 5-$HT_{2\beta Pan}$ receptor-mediated changes in cf.

Representative experiments are shown for cinanserin (Fig. 5*A*, $n = 8$) and (+)butaclamol (Fig. 5*B*, $n = 22$). In these serial experiments, modulatory input was blocked with sucrose on the *stn* and the preparation stabilized in a basal cycling state for 1 h. Baseline measurements of cf were obtained immediately before a 5-min application of 10 μM 5-HT (labeled 5-HT baseline in Fig. 5). 5-HT application was followed by a 1-h wash. Since baseline increased and remained steadily elevated throughout these experiments (Figs. 2*D* and 3*A*), a new baseline (labeled antagonist baseline in Fig. 5) was measured immediately before application of antagonist and represented the last 10 cycles of the 1-h wash. Antagonist (10 μM) was applied alone for 5 min and then together with 10 μM 5-HT for 5 min followed by a 1-h wash. Antagonists alone had no significant effect on cf (mean cinanserin-induced change in cf = $-0.5 \pm 1.5\%$, $P > 0.7$, $n = 8$; mean (+)butaclamol-induced change in cf = $0.2 \pm 1.4\%$, paired *t*-test $P > 0.8$, $n = 22$).

Regardless of the network's initial response to 5-HT (e.g., F, S, NC), in about 91% of the experiments 5-$HT_{2\beta Pan}$ antagonists consistently altered the 5-HT–induced change in cf in two respects. First, the antagonist abolished the rise in cf usually observed during temporal phase 2 of the 5-HT response (see Fig. 3*C*). In the presence of 5-HT alone, cf increased during phase 2 relative to phase 1 in 26 of 30 experiments (average Δcf {phase 2 peak − phase 1 nadir} = 0.17 ± 0.04 Hz; paired *t*-test for Ph2 peak vs. Ph1 nadir $P < 10^{-3}$, $n = 30$). However, in the presence of 5-HT plus antagonist, the phase 2 peak was no longer significantly different from phase 1 nadir (average Δcf {phase 2 peak − phase 1 nadir} = -0.03 ± 0.05 Hz; paired *t*-test for Ph2 peak vs. Ph1 nadir $P > 0.56$, $n = 30$). Second, whereas 5-HT alone produced no significant change in mean steady-state 5-HT cf relative to baseline (see Fig. 1*D*), 5-HT plus antagonist produced a significant decrease in mean steady-state 5-HT cf relative to baseline (mean steady-state cf in 5-HT plus antagonist/baseline = $0.67 + 0.05$, paired *t*-test $P < 10^{-7}$, $n = 30$). When considered in light of the fact that 5-$HT_{2\beta Pan}$ receptors have been localized to the STG neuropil (Clark et al. 2004), these data suggest that 5-$HT_{2\beta Pan}$ receptors are part of the 5-HT response system that modulates cf in most preparations. However, because pharmacology across paralogs within a class (e.g., 5-$HT_{2\alpha}$ and 5-$HT_{2\beta}$) is often conserved (Saudou et al. 1992), we cannot conclude that the antagonists are acting solely on 5-$HT_{2\beta Pan}$ receptors. For this reason we will refer to the component blocked by 5-$HT_{2\beta Pan}$ antagonists as the 5-$HT_{2\beta Pan}$-like component.

In Fig. 5, application of antagonist plus 5-HT appeared to restore the preparation to its original, pre-5-HT cf (i.e., 5-HT baseline). Based on this figure one might speculate that the second drug application removed a long-lasting change initiated by the first 5-HT application. Several pieces of evidence suggest that this is not the case: First, the change in cf elicited by antagonist plus 5-HT did not vary according to whether the drugs were applied directly to a naive preparation ($n = 5$) or followed a prior exposure to 5-HT and a 1-h wash (Fig. 5), and the drug-induced changes from baseline resulting from these two types of applications were not significantly different ($P = 0.77$). Second, there was no correlation between "5-HT baseline − antagonist baseline" and "antagonist baseline − cf in 5-HT plus antagonist" (linear regression, $P > 0.8$, $n = 30$). Third, there was no significant correlation between 5-HT baseline and steady-state cf in 5-HT plus antagonist (linear regression, $P = 0.07$, $n = 30$).

At least two highly variable components comprise the 5-HT response system

The experiments represented in Fig. 5 suggested that at least two independent components comprised the 5-HT response system that regulated cf: a 5-$HT_{2\beta Pan}$-like component that was lost on antagonist application and a non-5-$HT_{2\beta Pan}$ component that remained on antagonist application. We selected 24 of the original 30 antagonist experiments that were relatively periodic throughout the recording interval and computationally isolated their 5-$HT_{2\beta Pan}$-like components. Importantly, we have shown that 5-HT receptors respond in a like manner to serial 5-min applications of 5-HT spaced at 1-h intervals (Fig. 3*B*). Thus for each experiment we could approximate and visualize the 5-$HT_{2\beta Pan}$-like component of the 5-HT–induced change in cf as a difference trace obtained by subtracting the cf plots acquired in the presence versus the absence of antagonist, as described in METHODS. A subset of our 24 analyses that reflects the range of observed variability is shown in Fig. 6. This figure makes the point that the 5-HT–induced change in cf (blue trace in *left panels*, termed *blue trace average*; see METHODS) is composed of at least two separable and highly distinct components, a 5-$HT_{2\beta Pan}$-like component (gold trace in *right panels*, termed *difference trace*; see METHODS) and a non-5-$HT_{2\beta Pan}$ component (green trace in *left panels*, termed *green trace average*; see METHODS), which can perhaps be further subdivided (see following text). Note that any synergistic effects resulting from the interaction between the components would be lost on application of the 5-$HT_{2\beta Pan}$ antagonist, and therefore attributed solely to the 5-$HT_{2\beta Pan}$-like component. Unfortunately, despite a considerable effort, we could not identify specific 5-$HT_{2\beta Pan}$ agonists to complement the antagonist studies.

Figure 7 shows the average response for all 24 preparations (Fig. 7, *A–C*) and a quantification of the variability between the 24 preparations (Fig. 7, *D–F*). The mean of the 24 individual blue trace averages is plotted in Fig. 7*A*. The three previously described temporal phases of the 5-HT response are demarcated. To quantify the response for an individual preparation, we measured the change from baseline during each of the three temporal phases as described in METHODS. The 24 individual preparations are plotted as 24 blue circles in 3-D space in Fig. 7*D*. Each axis represents one of the three temporal phases. For a given axis (temporal phase), numbers >1 or <1 represent an increase or decrease in cf relative to baseline, respectively. The larger the change, the further the datum is from the number 1. The means and the individual variability for the non-5-$HT_{2\beta Pan}$ com-

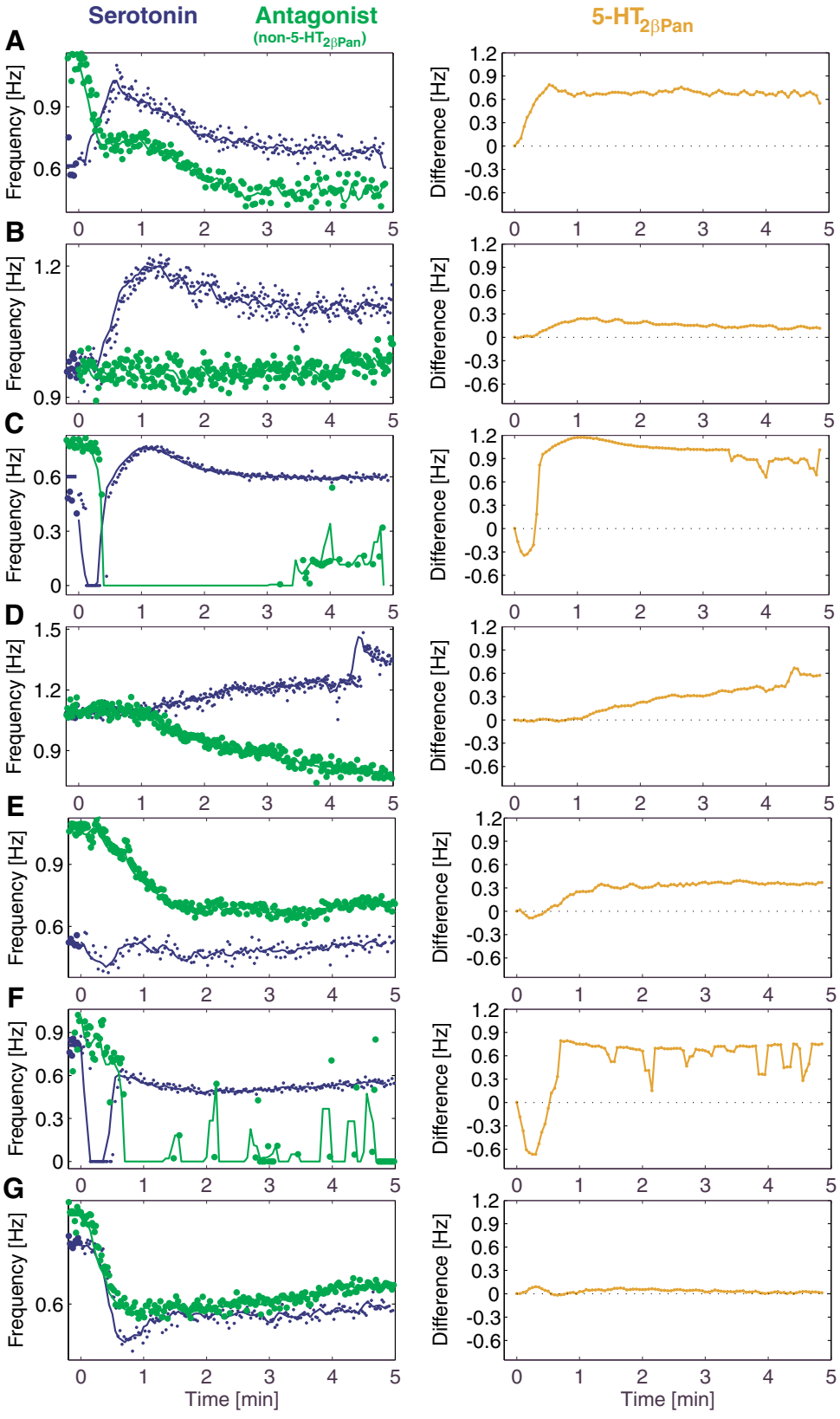

FIG. 6. Examples of the computationally isolated 5-$HT_{2\beta Pan}$-like component of the 5-HT response system. Cycle frequency time-course plots for 7 different preparations are shown (*A–G*). These experiments are representative of the 24 preparations analyzed. For a given experiment, the frequency plot obtained in 10 μM 5-HT is shown in blue and the frequency plot obtained in 10 μM 5-HT + 10 μM 5-$HT_{2\beta Pan}$ antagonist is shown in green. Each point represents a single cycle and lines indicate the trace averages as described in METHODS. In many cases the trace average is such an accurate fit that it is difficult to distinguish from the row data. The gold trace on the *right* is the difference trace obtained by subtracting the response to 5-HT in the presence of antagonist (green trace average) from the 5-HT response (blue trace average) after arbitrarily setting both baselines to zero.

ponent (Fig. 7, *B* and *E*, respectively) and the 5-$HT_{2\beta Pan}$-like component (Fig. 7, *C* and *F*, respectively) are similarly plotted. There were statistically significant correlations between the amplitudes of the changes in cf relative to baseline during the three temporal phases (e.g., phase 1 cf/baseline vs. phase 2 cf/baseline). It appeared that the larger the decrease in cf during phase 1, the smaller the increase over baseline in phases 2 and 3 ($P < 0.05$, correlation analysis, Prism).

Whereas the 5-$HT_{2\beta Pan}$-like component was largely responsible for a delayed, sustained increase in cf relative to baseline

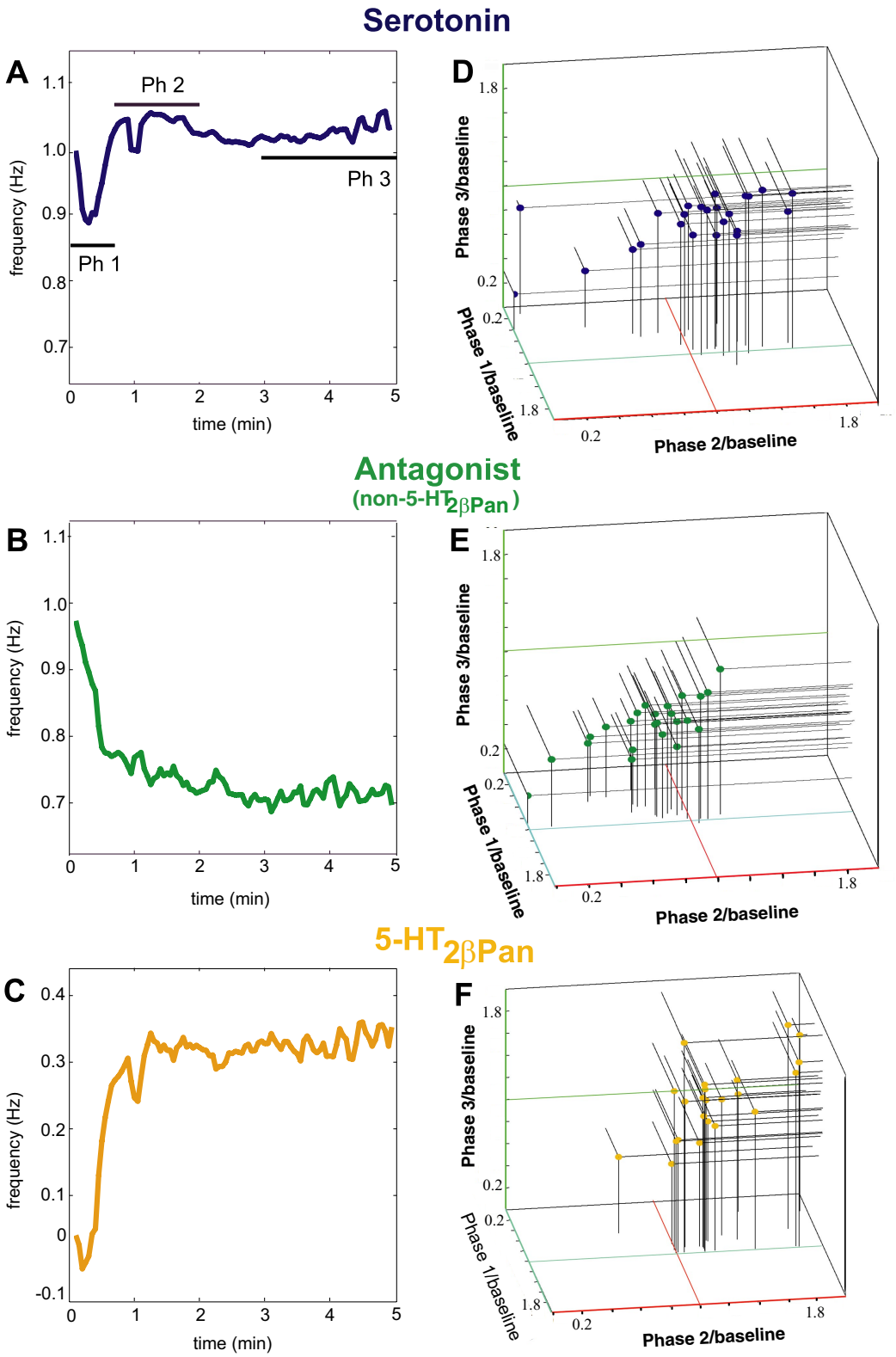

FIG. 7. Average 5-HT–induced changes in cycle frequency are underpinned by significant individual variation in the 5-HT$_{2\beta Pan}$-like and non-5-HT$_{2\beta Pan}$ components of the 5-HT response system. The same 24 experimental preparations are represented in all panels. The *left panels* show the mean of the 24 trace averages for preparations treated with10 μM 5-HT (*A*) or with 10 μM 5-HT + 10 μM antagonist (*B*), or the mean of the 24 difference traces (*C*). The 3 temporal phases of the response are indicated in *A*. The *right panels* show the distribution in 3-dimensional space of 5-HT–induced changes in cycle frequency relative to baseline for individual preparations in the absence (*D*) or presence (*E*) of antagonist, or for their computationally isolated 5-HT$_{2\beta Pan}$-like component (*F*). The 3 dimensions represent the 3 temporal phases of the 5-HT response. The black lines emanating from each circle simply help to portray the exact location of each individual preparation in 2-dimensional space. The colored lines in *D–F* indicate the number 1 on each axis.

(Fig. 7*C*), there was a remarkable amount of preparation-to-preparation variability in this component (Figs. 6 and 7*F*). In 2 of the 24 experiments, the 5-$HT_{2\beta Pan}$-like component was comparatively small or absent (e.g., Fig. 6*G*). In the remaining 22 experiments the difference trace was typically biphasic, such that 5-$HT_{2\beta Pan}$-like receptor activation generally produced an initial decrease in cf during temporal phase 1, followed by a slower increase that peaked during temporal phase 2 and attained a steady state by 5 min (i.e., phase 3). In some experiments, however, one or more of these attributes of the 5-$HT_{2\beta Pan}$-like component were absent. For example, the trough in temporal phase 1 was missing in the experiment shown in Fig. 6*A*, and both the trough and steady-state phases were missing in *experiment* 6*D*. Despite this variability, the mean nadir in phase 1 and peaks in phases 2 and 3 were significantly different from baseline (mean cf/baseline ± SD = 0.76 ± 0.43, 1.51 ± 0.33, and 1.26 ± 0.45 Hz; paired *t*-test, $P < 0.05$; $n = 24$). Note that the calculated mean phase 1 nadir for the 5-$HT_{2\beta Pan}$-like component (−0.24) differs from that which is graphed in Fig. 7*C* (more than −0.1). This is because the exact time of the nadir varied with each preparation (e.g., see Fig. 6) so that when all difference traces were averaged, the large nadirs seen in individual preparations were smoothed away in the average and thereby obscured. This is also true to a lesser extent for the phase 2 peak.

The non-5-$HT_{2\beta Pan}$ component produced an immediate and sustained decrease in cf relative to baseline (Fig. 7*B*). In some cases the initial decrease in cf could be followed by a small, gradual increase (e.g., Fig. 6, *C* and *G*). In 3 of the 24 experiments the non-5-$HT_{2\beta Pan}$ component was absent (e.g., Fig. 6*B*). In other experiments there was an obvious shift in the time constants of decay between 30 s and 2 min (e.g., Fig. 6*A*), and in 6 of 24 experiments there was an obvious increase in cf during this period. Whereas an unknown element may mediate the increase, it is also possible that the 5-$HT_{2\beta Pan}$-like component was incompletely blocked by antagonist in these preparations. Although variable, the mean decrease in cf relative to baseline for the non-5-$HT_{2\beta Pan}$ component was statistically significant during all three temporal phases [mean cf/baseline + SD = 0.79 ± 0.19 Hz (Phase 1), 0.77 ± 0.31 Hz (Phase 2), and 0.71 + 0.22 Hz (Phase 3), $n = 24$, paired *t*-test, $P < 10^{-3}$].

It might be questioned whether some or all of the variability in the response to 5-HT results from the response being sensitive to absolute cf immediately before modulator application. For example, in the crab STNS, the crustacean cardioactive peptide (CCAP) hormone consistently increased cycle period during a relatively fast gastric mill rhythm, but produced inconsistent results during slower rhythms (Kirby and Nusbaum 2007). Figures 1*C* and 2 suggest that the steady-state 5-HT effect is not sensitive to baseline cf. We further examined the cycle-period–dependent effects of 5-HT in all phases of the 5-HT response and for the two individual components by performing correlation analyses (Prism, GraphPad) on measurements from these 24 preparations. Baseline frequency versus the 5-HT–induced change in cf [i.e., (cf in 5-HT)/baseline] for each of the three temporal phases in each of the 24 preparations was plotted. None of the three correlations was significant ($P > 0.05$). We performed similar analyses for each temporal phase of the non-5-$HT_{2\beta Pan}$ component [i.e., antagonist baseline vs. (cf in antagonist + 5-HT)/antagonist baseline] and the 5-$HT_{2\beta Pan}$-like component (baseline vs. difference trace measurements) and found no significant correlations ($P > 0.05$ in all cases). Thus the actions of 5-HT appear to be independent of absolute cf in all three temporal phases of the response, even at the level of individual components.

Sum of the two opposing and variable components determines the class

As discussed at the beginning of RESULTS, preparations could be divided into three classes depending on whether cf increased (F), decreased (S), or remained unchanged (NC) relative to baseline after 5 min in 5-HT. Comparisons of the three classes with a one-way ANOVA followed by a Tukey post hoc test demonstrated that all classes were significantly different from each other at steady state (Table 3, last three columns, phase 3). Interestingly, one-way ANOVAs indicated that there were no significant differences in cycle frequencies between these classes prior to 5-HT application ($P > 0.6$ for intact preparations; $P > 0.85$ for preparations with a sucrose block on the *stn*; data not shown). These data indicate that circuits that do not appear to be functionally different (e.g., similar cycle frequencies across individuals) can show different responses to the same modulatory challenge.

The existence of the three classes could be due to class-specific differences in the components of the 5-HT response system (e.g., the 5-$HT_{2\beta Pan}$-like component that increases cf is always large in Class F and small in Class S). To address whether there were fundamental differences in the 5-$HT_{2\beta Pan}$-like component between the three classes, we used one-way ANOVAs to compare the changes in cf produced by 5-$HT_{2\beta Pan}$-like receptor activation during a given temporal phase. Table 3 shows that there were no significant differences in the 5-$HT_{2\beta Pan}$-like component between

TABLE 3. *Average 5-HT-induced fold change relative to baseline in each phase of a given class*

	5-$HT_{2\beta Pan}$–Like Component cf/Baseline			Non-5-$HT_{2\beta Pan}$ Component (cf in 5-HT + Antagonist)/Baseline			Complete 5-HT Response System (cf in 5-HT)/Baseline		
Class (*n*)	F (11)	S (7)	NC (6)	F (11)	S (7)	NC (6)	F (11)	S (7)	NC (6)
Phase 1	0.86 ± 0.07	0.74 ± 0.09	0.89 ± 0.05	0.86 ± 0.04	0.67 ± 0.08	0.72 ± 0.09	0.98 ± 0.03#†	0.56 ± 0.10*	0.67 ± 0.06*
Phase 2	1.40 ± 0.09	1.15 ± 0.16	1.27 ± 0.07	0.81 ± 0.10	0.65 ± 0.10	0.70 ± 0.014	1.31 ± 0.06#	0.62 ± 0.18*	1.05 ± 0.06
Phase 3	1.44 ± 0.08	1.08 ± 0.12	1.40 ± 0.10	0.73 ± 0.07	0.62 ± 0.09	0.67 ± 0.04	1.22 ± 0.04#†	0.64 ± 0.09*†	0.98 ± 0.01*#

Values are means ± SE for the 5-$HT_{2\beta Pan}$–like component, the non-5-$HT_{2\beta Pan}$ component, and the total response. The 5-HT–induced change from baseline during each temporal phase was calculated as described in METHODS for each of the 24 preparations represented in Figs. 6 and 7. Significant differences between classes were determined for each component or the total response, by comparing preparations using one-way ANOVAs followed by Tukey post hoc tests. We compared data representing only the same temporal phase and the same component (i.e., three adjacent rows). Note that there were no differences in phases 1, 2, or 3 of the 5-$HT_{2\beta Pan}$–like component between classes F, S, and NC. Similarly, there were no significant differences in the non-5-$HT_{2\beta Pan}$ component between classes during temporal phases 1, 2, or 3. However, significant differences between classes could be observed for the total 5-HT response during all three temporal phases. *, significantly different from Class F, $P < 0.05$; #, significantly different from Class S, $P < 0.05$; †, significantly different from Class NC, $P < 0.05$.

the different Classes for any temporal phase. This can also be seen by examining Fig. 6. For example, the preparations in Fig. 6, *C* and *F* belong to Classes F and S, respectively, and yet they have highly similar 5-$HT_{2\beta Pan}$-like components. Comparable analyses indicated that neither were there statistically significant differences in the non-5-$HT_{2\beta Pan}$ component between the classes (Table 3, Fig. 6). In sum, the two components displayed preparation-to-preparation variability within a class; however, when all preparations were considered, the set of components in one class was no different from that in another, and a given component (e.g., producing large vs. small change from baseline) was equally likely to be found in any of the three classes.

How are different classes of responses produced from the same set of components? Analyses of individual preparations suggested it was the balance of the two components that determined the class. At steady-state 5-$HT_{2\beta Pan}$-like > non-5-$HT_{2\beta Pan}$ for Class F, non-5-$HT_{2\beta Pan}$ > 5-$HT_{2\beta Pan}$-like for Class S, and non-5-$HT_{2\beta Pan}$ = 5-$HT_{2\beta Pan}$-like for Class NC.

Figure 6 shows that the 5-HT–induced change in cf was the sum of two highly variable components. Initially both components produced a decrease in cf. The minima of the two components were not necessarily coincident. Whereas the non-5-$HT_{2\beta Pan}$ component continued to decrease throughout phase 1, the 5-$HT_{2\beta Pan}$-like component reached its nadir and then began to rise late in phase 1. From this point on the two components produced opposing changes in cf, and their balance appeared to determine whether 5-HT ultimately produced a net increase, decrease, or no change in cf relative to baseline. This is most clearly seen by comparing Fig. 6, *B*, *E*, and *F*. One of the largest 5-$HT_{2\beta Pan}$-like components is observed in Fig. 6*F* (~0.9-Hz increase at steady state), but in this experiment 5-HT produced a 32% net decrease in cf at steady state because the non-5-$HT_{2\beta Pan}$ component was even larger. The experiment shown in Fig. 6*B* has the smallest 5-$HT_{2\beta Pan}$-like component (~0.15-Hz increase at steady state), but 5-HT produced a significant 14% net increase at steady state because the non-5-$HT_{2\beta Pan}$ component was absent. Figure 6*E* shows an intermediate 5-$HT_{2\beta Pan}$-like component (~0.4-Hz increase at steady state), yet 5-HT had no net effect on cf in this experiment because the non-5-$HT_{2\beta Pan}$ component was equally large. Thus the steady-state 5-HT response is determined by the sum of opposing components.

This idea that each class represents a different balance of components is further substantiated by an examination of the means within a class. In Class F the average 5-$HT_{2\beta Pan}$-like component was about 1.6-fold larger than the average non-5-$HT_{2\beta Pan}$ component at steady state (mean % change from baseline cf at steady state produced by each component: 5-$HT_{2\beta Pan}$-like = 44 ± 8% increase, non-5-$HT_{2\beta Pan}$ = 27 ± 8% decrease, $n = 11$), but the opposite was true for Class S preparations (mean % change from baseline cf at steady state produced by each component: 5-$HT_{2\beta Pan}$-like = 8 ± 12% increase, non-5-$HT_{2\beta Pan}$ = 38 ± 9% decrease, $n = 7$). Further, using the aforementioned measurements of the 5-HT–induced change from baseline during phase 3 (see Fig. 7, *E* and *F*) we obtained a ratio of the components for each preparation at steady state (phase 3 5-$HT_{2\beta Pan}$-like component/phase 3 non-5-$HT_{2\beta Pan}$ component). A Kruskal–Wallis followed by a Dunnett's post hoc test showed that the ratios were significantly different for Classes F and S (Table 4). Together these analyses suggest that the different classes represent a change in the balance of opposing components of the 5-HT response system.

TABLE 4. *Average component ratios at steady state (phase 3)*

5-$HT_{2\beta Pan}$–Like Component (Hz)/Non-5-$HT_{2\beta Pan}$ Component (Hz)		
Class F (11)	Class S (7)	Class NC (6)
3.74 ± 1.75#	0.55 ± 0.16*	1.19 ± 0.18

Values represent the means (±SE) of the ratios for each class. For each of the 24 individual preparations analyzed and represented in Figs. 6 and 7, the ratio of the 5-$HT_{2\beta Pan}$ component to the non-5-$HT_{2\beta Pan}$ component was obtained at steady state. Significant differences in the ratios between the three classes were determined with a Kruskal–Wallis, followed by a Dunnett's post hoc test. *, significantly different from Class F, $P < 0.05$; #, significantly different from Class S, $P < 0.05$.

5-$HT_{1\alpha Pan}$-like receptors mediate a slow increase in cf

We next examined the role of 5-$HT_{1\alpha Pan}$ receptors in mediating the 5-HT effect on cf. Because we were unable to identify specific antagonists for 5-$HT_{1\alpha Pan}$, we used an agonist, mCPP, to investigate the role of this receptor. Although mCPP is a relatively weak agonist of 5-$HT_{1\alpha Pan}$, it was the only one tested that had no activity at 5-$HT_{2\beta Pan}$ in cell culture (Table 1). This criterion was important since 5-$HT_{2\beta Pan}$ activation contributed significantly to 5-HT–induced changes in cf (Figs. 5–7). In these studies 100 μM mCPP was used to activate 5-$HT_{1\alpha Pan}$ receptors because 10–50 μM mCPP was ineffective (Zhang and Harris-Warrick 1994; Spitzer, unpublished). Given the high concentration of mCPP used, we cannot rule out the action of this drug at other receptors. Thus the component of the 5-HT response system identified by these experiments will be referred to as the 5-$HT_{1\alpha Pan}$-like component.

Figure 8*A* shows an example of a typical mCPP experiment. In this preparation a 5-min, 5-HT (10 μM) application slowed cf. 5-HT application was followed by a 1-h wash and a 5-min application of 100 μM mCPP. After a further 1-h wash, (+)butaclamol, a 5-$HT_{2\beta Pan}$ antagonist, was applied for 5 min followed by butaclamol ± mCPP. In some experiments the orders of 5-HT and mCPP applications were reversed.

Application of mCPP caused an increase in cf in all preparations regardless of the 5-HT effect. Figure 8*B* illustrates that the mean steady-state cf, measured as the average during the last minute of mCPP application, significantly increased by 33 ± 4.5% relative to baseline. The time course of the response varied so that the peak effect was reached between 1 and 5 min. In seven of nine experiments, a steady state was reached within 5 min, and in the remaining two preparations the cf continued to increase throughout the 5-min 5-HT application. The mCPP-induced increase was not blocked by (+)butaclamol, and its magnitude varied across preparations by a factor of 5. After a 1-h washout of mCPP, there was an increase in cf relative to baseline, similar to preparations exposed to 5-HT. As shown in Figs. 2*D* and 3*A*, this increase could be due to mCPP-independent phenomena. Reversing the order of 5-HT and mCPP applications did not alter the observed effects.

These data suggest that 5-$HT_{1\alpha Pan}$-like receptors could contribute a small, gradual increase in cf to the non-5-$HT_{2\beta Pan}$ component of the 5-HT response system. Unfortunately, the lack of a specific 5-$HT_{1\alpha Pan}$ antagonist prevented us from testing this hypothesis further. However, if this hypothesis is true, then there must be at least one additional subcomponent that mediates a decrease in cf and opposes both the increases mediated by 5-$HT_{1\alpha Pan}$-like and 5-$HT_{2\beta Pan}$-like receptors at steady state.

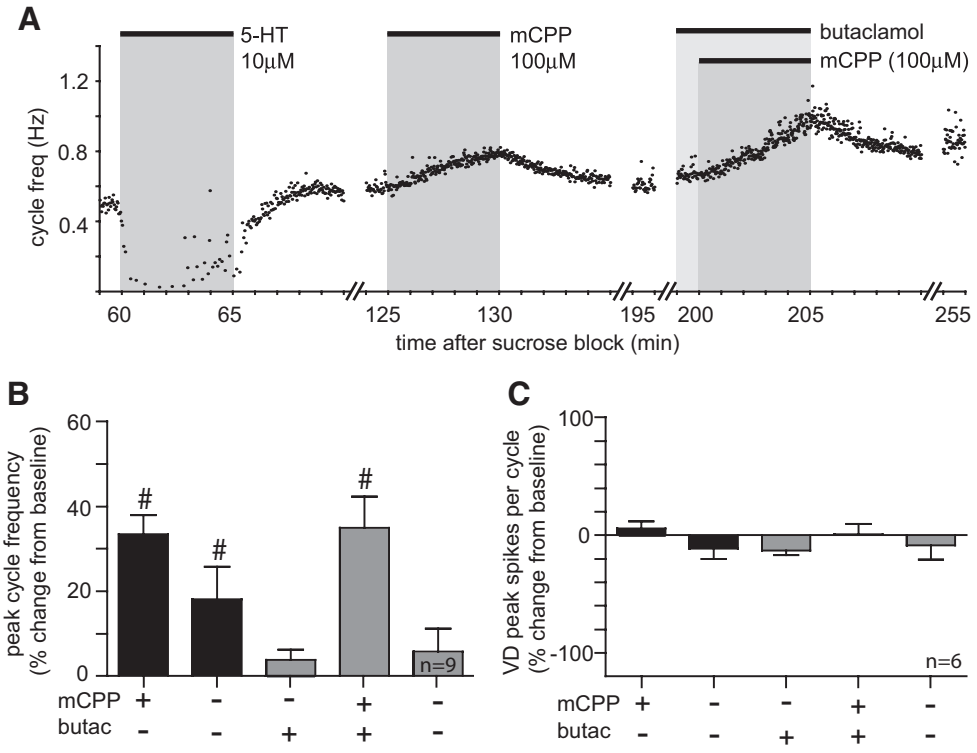

FIG. 8. Cycle frequency may be increased via activation of 5-$HT_{1\alpha Pan}$. Serotonergic inhibition of VD does not occur via 5-$HT_{1\alpha Pan}$. *A*: application of 100 μM 1-(*m*-chlorophenyl)-piperazine (mCPP), a 5-$HT_{1\alpha Pan}$ agonist, results in an increase of peak cycle frequency regardless of the individual preparation's response to 5-HT. In this example, 10 μM 5-HT application results in a significant slowing of the rhythm (*left*). When mCPP is applied, however, the cycle frequency is increased (*middle*). This increase is not affected by the 5-$HT_{2\beta Pan}$ blocker (+)butaclamol (10 μM, *right*). *B*: 100 μM mCPP significantly increases peak cycle frequency. Bar graphs indicate the average percentage change in cycle frequency during sequential application of drugs [(cycle frequency/baseline) $\times$ 100]. Error bars indicate the SE. The presence (+) or absence (−) of a given drug is as indicated underneath each bar. Conditions in which both drugs are absent indicate the first and second washouts. The mCPP effect is not changed in the presence of the 5-$HT_{2\beta Pan}$ blocker, (+)butaclamol. *C*: VD spiking is not changed by mCPP applications. Bar graphs indicate the average percentage change in VD spike frequency during sequential application of drugs [(spike frequency/baseline) $\times$ 100]. Error bars indicate the SE. The presence (+) or absence (−) of a given drug is as indicated underneath each bar. Washes are indicated as (−/−). In the case of the first wash, the bar represents the difference between the first and second baselines. Paired *t*-test, #$P < 0.05$ vs. baseline.

5-HT effects on VD could underpin the decrease in cf associated with the non-5-$HT_{2\beta Pan}$ component

In the intact system, VD is thought to regulate cf via its rectifying electrical junctions with the pacemaker kernel. It was previously shown that VD acts to increase cf, most likely by injecting positive current into the AB/PD pacemaker during the depolarizing phase of the pacemaker oscillation (Weaver and Hooper 2003). VD's governance of cf is state dependent, such that VD's influence is greatest at slower cycle frequencies (e.g., $\leq$1.0), which are typical for the deafferented preparations studied here (Fig. 1*D*; average baseline cf = 0.77 + 0.4 Hz, $n = 44$). In the absence of 5-HT, VD is active in deafferented preparations (Fig. 1*B*, *mvn trace, middle*); thus it is likely that VD provides an accelerating influence on cf under these experimental conditions. Presumably, phenomena that inhibit VD and/or reduce its electrical coupling with the pacemaker kernel will diminish VD's accelerating influence on the pacemaker, and thereby slow cf. It was previously shown that *1*) 10 μM 5-HT reduces the electrical coupling between VD and the pacemaker kernel by about 50% (Johnson et al. 1993); *2*) 10 μM 5-HT normally hyperpolarizes VD by −10 mV to inhibit firing (Flamm and Harris-Warrick 1986b; see also Fig. 1*B, mvn trace, bottom*); and *3*) all else being equal, a −10-mV hyperpolarization of VD can reduce cf by 35–86% (Weaver and Hooper 2003). The typical time course for the 5-HT–induced change in VD firing frequency, shown in Fig. 9*A*, corresponds to that for the non-5-$HT_{2\beta Pan}$ component of the 5-HT response system (e.g., compare green traces in Figs. 6 and 7 with Fig. 9*A*). Moreover, none of the 5-$HT_{2\beta Pan}$ antagonists had any effect on the VD neuron's response to 5-HT (Fig. 9, *B* and *C*); and application of mCPP, a 5-$HT_{1\alpha Pan}$ agonist, also did not alter the firing rate of the VD neuron (Fig. 8*C*). Thus neither 5-$HT_{2\beta Pan}$-like nor 5-$HT_{1\alpha Pan}$-like receptors mediate the 5-HT–induced hyperpolarization of VD. Together these data suggest that 5-HT effects on VD could produce the rapid and sustained decrease in cf associated with the non-5-$HT_{2\beta Pan}$ component of the 5-HT response system.

5-$HT_{2\beta Pan}$-like receptors do not mediate the excitation of IC

The activity of the IC cell is visible on many *mvn* recordings. Like LP, IC was silent after the sucrose block was applied. However, consistent with previous studies (Flamm and Harris-Warrick 1986a), in some preparations 5-HT elicited spikes in the IC. The 5-$HT_{2\beta Pan}$ antagonists had no effect on 5-HT–induced excitation of IC in any preparation regardless of whether 5-HT produced an increase ($n = 8$; data not shown) or decrease in cf ($n = 5$; not shown). Thus 5-$HT_{2\beta Pan}$-like receptors do not mediate the 5-HT–induced excitation of IC.

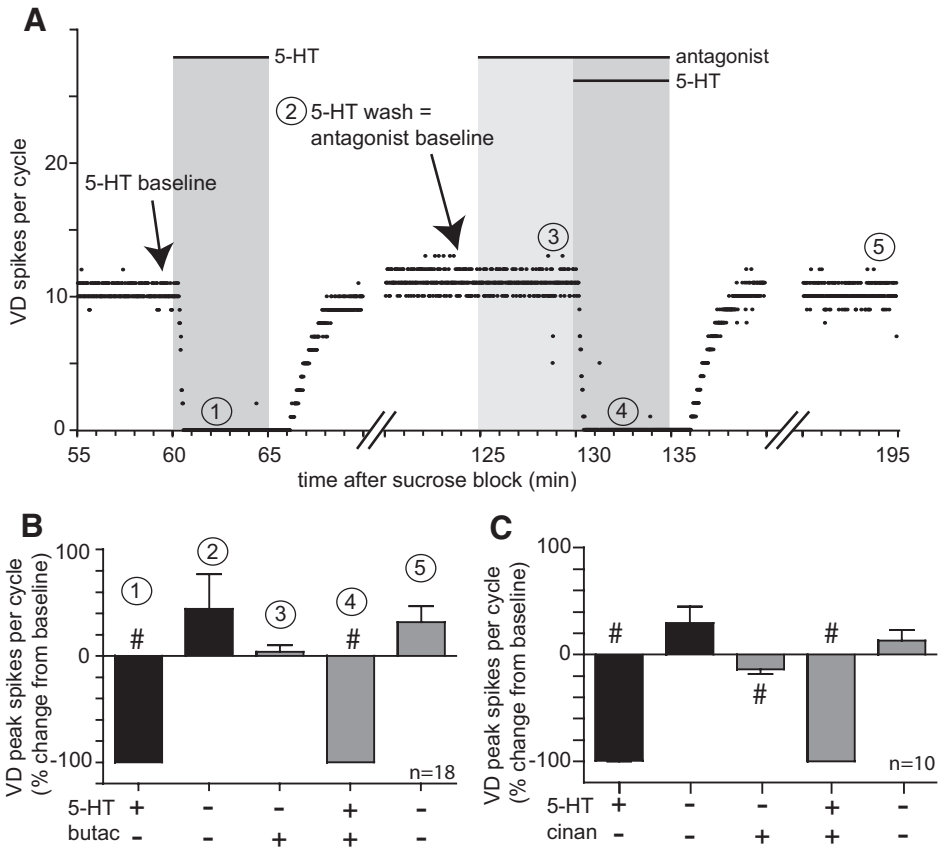

FIG. 9. 5-HT$_{2\beta Pan}$ is not involved in elimination of VD activity by 5-HT. *A*: time course graph of a representative experiment showing VD spikes per cycle during serial application of 10 μM 5-HT followed by 10 μM antagonist alone and with 10 μM 5-HT. Serial applications are separated by 1 h of wash. Circled numbers correspond to time points for measurements presented in bar graphs below. Spiking in the VD neuron is completely inhibited in 10 μM 5-HT. This effect is not blocked by either (+)butaclamol (*B*) or cinanserin (*C*). Bar graphs in *B* and *C* indicate the average percentage change in VD spike frequency during sequential application of drugs [(spike frequency/baseline) $\times$ 100]. Note that the baseline is reset between bars 2 and 3. Error bars indicate the SE. The presence (+) or absence (−) of a given drug is as indicated underneath each bar. Washes are indicated as (−/−). In the case of the first wash (circle 2), the bar represents the difference between the first and second baselines (paired *t*-test, #$P < 0.05$ vs. baseline).

DISCUSSION

To reconcile the emerging principles of plasticity (Davis 2006) and metamodulation (Katz and Edwards 1999) with network stability (discussed in Marder and Goaillard 2006; Nowotny et al. 2007), we have deconstructed the 5-HT response system that controls pyloric network cycle frequency (cf). We found that the system was composed of at least three separable components. Some of the components produced opposing changes in cf and each component showed a great deal of preparation-to-preparation variability. In the absence of all other modulatory inputs, this system produced a variable response to 5-HT. Ultimately, the balance of opposing components determined whether 5-HT produced an increase, decrease, or no change in cycle frequency.

Three components of the 5-HT response system

Our data suggest that there are at least three distinct components of the 5-HT response system controlling cf. The first component is associated with a 5-HT$_{2\beta Pan}$-like transduction cascade(s). This component is characterized by an initial decrease followed by a steady-state increase in cf. The biphasic response most likely reflects activation of distinct signaling pathways on different timescales. 5-HT$_{2\beta Pan}$ receptors couple with Gq to activate phospholipase Cβ and ultimately increase the activity of protein kinase C in HEK cells (Clark et al. 2004). In mammals, activation of the 5-HT$_2$ family can additionally stimulate phospholipase A$_2$, NO synthesis, and the MAP kinase cascade (Nebigil et al. 2001). It is not clear whether the mechanism giving rise to the bimodal effect involves one or a combination of these (or other) signaling pathways.

Differential localization of the receptor could also contribute to bimodality. Arvanov et al. (1999) showed that 5-HT$_{2A}$ receptors generated a biphasic response in rat medial prefrontal cortex because they were located both pre- and postsynaptically. The subcellular compartmentalization of 5-HT$_{2\beta Pan}$ receptors within the synaptic neuropil of the STG is not known. All STG neurons express 5-HT$_{2\beta Pan}$, and this receptor is found throughout the synaptic neuropil, but not in the plasmalemma surrounding the soma or large-diameter neurites (Clark et al. 2004). We previously demonstrated that 5-HT$_{2\beta Pan}$ receptors were located on distal axon terminals in PD and PY cells (Clark et al. 2004). Here we have shown that 5-HT$_{2\beta Pan}$ receptors do not mediate 5-HT inhibition of VD or excitation of IC; hence, 5-HT$_{2\beta Pan}$ receptors may also be localized to the peripheral regions of these neurons. 5-HT is known to regulate multiple conductances in the AB pacemaker neuron, ultimately enhancing its excitability and synaptic output to increase steady-state cf (Flamm and Harris-Warrick 1986b; Harris-Warrick and Flamm 1987; Johnson et al. 1993;). Furthermore, the 5-HT$_{2\beta Pan}$ antagonist cinanserin blocks 5-HT–elicited AB/PD bursting in the crab, *Cancer borealis* (Zhang and Harris-Warrick 1994). The most parsimonious interpretation of all the data is that the 5-HT$_{2\beta Pan}$-like receptors responsible for increasing steady-state cf reside in the AB synaptic neuropil. However, it is also possible that these receptors reside on the terminals of modulatory projection neurons, and that some of the varied effects of 5-HT on cf are mediated by local interactions between these terminals and their targets (Coleman and Nusbaum 1994; Coleman et al. 1992; Goaillard et al. 2004).

The second component of the 5-HT response system is mediated by a 5-HT$_{1\alpha Pan}$-like transduction cascade. This com-

ponent produces a small, gradual increase in cf. 5-$HT_{1\alpha Pan}$ receptors couple with Gi/o in HEK cells to decrease cAMP (Spitzer et al. 2008). The location of this receptor is presently unknown, although it is unlikely to be found in the VD synaptic neuropil because the 5-$HT_{1\alpha Pan}$ agonist did not affect VD activity.

The third component of the 5-HT response system results in an immediate and sustained decrease in cf, but the receptors involved are currently unknown. The three uncharacterized GPCRs in the arthropod genome are unlikely candidates because they are not homologous to known 5-HT receptor subtypes (Clark and Baro 2007). We have shown here that this component is independent of 5-HT_1- and 5-HT_2-like receptors. The only remaining known arthropod 5-HT receptor is 5-HT_7, which couples with Gs (Schlenstedt et al. 2006).

Our results are consistent with the notion that the third component is at least partially localized to the VD follower neuron. However, this idea is called into question by Ayali and Harris-Warrick (1999), who showed that when modulatory inputs were intact, the 5-HT–induced change in cf was not significantly different between the isolated AB neuron, the isolated AB–PD pacemaker kernel, and the intact network. This suggested that 5-HT acted solely on the AB neuron to control cf. Interestingly, in their hands 5-HT always produced an increase in cf. A major difference between the two studies was the presence (Ayali and Harris-Warrick) versus the absence (this manuscript) of descending modulatory inputs. It is noteworthy that when modulatory inputs to the network are intact (i.e., nondeafferented preparation), LP and VD are both active and have reciprocal effects on cf (Weaver and Hooper 2003), and that 5-HT acts directly to hyperpolarize both LP and VD to the same extent (Flamm and Harris-Warrick 1986b). Conversely, in our deafferented preparation, LP is hyperpolarized prior to 5-HT application. Thus deafferentation may remove a fourth component of the 5-HT response system that resides on the LP and produces an increase in cf.

Sources of component variability

Our results are consistent with previous studies suggesting that similar network activity may be produced from disparate cell and network parameters (Bucher et al. 2005; Prinz et al. 2004). The most obvious sources for variability in the response to 5-HT are the proteins comprising the transduction cascades. Receptor function and/or expression can be state dependent (Ango et al. 2001; Anji et al. 2001; Bockaert et al. 2003; Cirelli and Tononi 2004; Clark and Baro 2007; Dwivedi et al. 2005; Riad et al. 2001; Spitzer et al. 2005; Wohlpart and Molinoff 1998). In addition, one or more downstream components of the 5-HT signal transduction cascades could vary. For example, alterations in the signaling pathway could occur at the level of the final target. In this regard, ion channel activity and expression in pyloric neurons are known to vary significantly across individuals (Golowasch et al. 1999; Schulz et al. 2006, 2007), and neuromodulatory input can regulate expression of ionic currents and channels over the long term (Khorkova and Golowasch 2007; Mizrahi et al. 2001).

Synaptic plasticity may also contribute to variability between preparations. 5-HT alters the strengths of glutamatergic synapses between the pacemaker kernel and follower LP and VD neurons, as well as electrical coupling between VD and the pacemaker kernel (Johnson and Harris-Warrick 1990; Johnson et al. 1993, 1994, 1995). In preliminary experiments, suppression of glutamatergic synapses did not prevent a variable 5-HT response. To our knowledge, the degree of preparation-to-preparation variability in the strength of electrical coupling between VD and the pacemaker kernel is presently unknown.

State-dependent effects that are independent of changes in gene expression and/or cell morphology could also account for the variability observed here. Many effects of G-protein–coupled receptors are made manifest only under certain conditions. For example, in prefrontal cortex neurons, activation of dopamine type 1 receptors (D1) significantly reduced excitatory postsynaptic potential decay time and integral at membrane potentials near spike threshold (i.e., upstate), but not at more hyperpolarized potentials (i.e., downstate). This is because D1 activation altered the phosphorylation state of Na^+ channels (Rotaru et al. 2007) at all membrane potentials (Carr et al. 2003), which altered voltage-dependent slow inactivation (Carr et al. 2003; Chen et al. 2006), such that Na^+ channel availability was reduced only in the upstate. Working on STG neurons, Nargeot (2003) demonstrated that the long-term effect of a neuromodulator could be consistent at the molecular level, and yet evoke opposite changes in neuronal activity depending on the cell's membrane potential. Similarly, state-dependent effects have been observed at the network level. For example, it has been shown that the influence of the same modulatory change (i.e., change in the strength of an identified synapse) can vary according to network cycle frequency (Thirumalai et al. 2006).

In sum, the variability we observed could be explained by a variety of mechanisms ranging from changes in gene expression to changes in ion channel phosphorylation states that alter membrane potential. With regard to the latter, it is important to note that the effects of endocrine and paracrine modulation can last well beyond the removal of their inputs (Blitz et al. 2008; Di Prisco et al. 1997; Turrigiano and Selverston 1990; Wood et al. 2004). This depends, in part, on the mechanisms for removal of neuroactive substances outside the synapse (Coleman et al. 1994; Wood and Nusbaum 2002), as well as the stability of the change induced by the modulator. Since we examined 5-HT actions roughly 2–4 h after removing hormonal inputs, and only 1 h after removing synaptic and paracrine modulatory inputs, their long-term actions could still be in effect.

Stability versus variability of neuromodulatory effects on STNS circuits

In direct contrast to our findings, there exists a vast literature (too large to fully cite here) documenting the reproducibility of neuromodulatory actions on STNS circuits. This apparent discrepancy is easily explained for work examining modulation by projection neurons onto circuit neurons (e.g., Saideman et al. 2007a; Stein et al. 2007) and/or extrinsic inputs onto these projection neurons (e.g., Beenhakker et al. 2007; Blitz et al. 2008). Since these types of studies usually use an intact preparation (i.e., nondeafferented), it may be that reproducibility is maintained through stabilizing mechanisms involving additional modulatory inputs and/or feedback from STG neurons to input neurons (Coleman and Nusbaum 1994; Coleman et al. 1995; Wood et al. 2004). The existence of these mechanisms was

implied in our studies by the fact that when we removed modulatory input, cycle frequency drifted over time. Additionally, projection/sensory neuron transmission can be highly targeted so that only one or a few components of a multicomponent system are activated by a given modulator (e.g., only the excitatory or the inhibitory components). Likewise, the apparent discrepancy is understandable for studies that bath-apply neuroactive substances to nondeafferented preparations (e.g., Krenz et al. 2000; Szucs et al. 2005); although the bath applied modulator would not be localized, the aforementioned stabilizing feedback mechanisms could still be in effect.

Considering only studies in which modulators were bath applied to deafferented preparations, one observes a large literature reporting reproducible effects of modulators on isolated ionic currents (e.g., Kloppenburg et al. 2000; Peck et al. 2001, 2006; Swensen and Marder 2000). These results are not inconsistent with our findings. In all of these studies the system was highly reduced to a single current in a synaptically isolated cell. Our work suggests that variability is diminished when examining individual components (e.g., VD inhibition) rather than the interaction of multiple components (e.g., network cf). It should be noted that in most studies of modulatory effects on ionic currents, individual differences in time courses and amplitudes could not be assessed because averages rather than individual responses were reported.

If we consider only those studies that involved bath application to deafferented preparations and that reported on cycle frequency, we find a few reports of variable neuromodulatory effects (e.g., Beltz et al. 1984; Saideman et al. 2007b); however, the majority of studies suggest that a given neuroactive substance reproducibly altered cycle frequency (e.g., Christie et al. 2006; Goaillard et al. 2004; Perez-Acevedo and Krenz 2005; Stemmler et al. 2007). Again, a lack of individual variability could not be verified due to the use of averages. One important difference between many of these studies and ours was that lower concentrations of a neuroactive substance were often used. This could account for the disparate findings because lower concentrations may activate fewer system components. For example, the EC_{50} for 5-HT at 5-$HT_{1\alpha Pan}$ is nearly an order of magnitude lower than that at 5-$HT_{2\beta Pan}$; thus at one extreme the 5-$HT_{1\alpha Pan}$ component might act alone, whereas at the other extreme both components could be maximally activated.

In sum, the paucity of reports on variable modulatory effects is intriguing. It might suggest that the 5-HT response system is more plastic than most neuromodulatory systems. Alternatively, it may be that variability in neuromodulatory response systems has been highly underestimated, perhaps due to reporting procedures and/or the use of techniques that examine individual components rather than their interactions.

Summary

It is becoming increasingly evident that variability in neuronal modulatory systems and networks is often the rule rather than the exception. In the absence of all other modulatory inputs, a given modulatory challenge will not have consistent actions on a cellular or circuit parameter if that parameter is a target of plasticity mechanisms (reviewed in Marder and Goaillard 2006). It is not known whether this variability occurs in vivo and, if so, what its functional significance might be. Presumably the variability could reflect adaptations of the stomatogastric network to changing digestive, life cycle, or environmental circumstances. Future investigations on this ideal preparation should provide substantial insight into how multiple modulatory, metamodulatory, and plasticity mechanisms are integrated to maintain an adaptive network.

ACKNOWLEDGMENTS

We thank Drs. Jack Peck and Anne Murphy for statistical advice, Drs. Jeffrey Triblehorn and Brian Antonsen for help with DataView and insightful discussions, J. Kim for excellent technical support, and M. Clark and the anonymous reviewers for critical reading of earlier versions of this manuscript and useful suggestions. We are deeply indebted to Dr. Wulf Krenz for building our physiology rigs those many years ago. N. Spitzer was a scholar in the Brains and Behavior Program and the Center for Behavioral Neuroscience at Georgia State University.

Present address of N. Spitzer: Department of Biology, College of Science, Marshall University, 1 John Marshall Drive, Huntington, WV 25755.

GRANTS

This work was supported by National Institutes of Health Grants DA-024039-01 to D. J. Baro and MH-62167 to D. H. Edwards and National Sciences and Engineering Research Council of Canada Grant PGS-D2-304455-2004 to N. Spitzer. Partial support came from the National Science Foundation under agreement IBN-9876754 to the Center for Behavioral Neuroscience.

REFERENCES

Ango F, Prezeau L, Muller T, Tu JC, Xiao B, Worley PF, Pin JP, Bockaert J, Fagni L. Agonist-independent activation of metabotropic glutamate receptors by the intracellular protein Homer. *Nature* 411: 962–965, 2001.

Anji A, Sullivan Hanley NR, Kumari M, Hensler JG. The role of protein kinase C in the regulation of serotonin-2A receptor expression. *J Neurochem* 77: 589–597, 2001.

Arvanov VL, Liang X, Magro P, Roberts R, Wang RY. A pre- and postsynaptic modulatory action of 5-HT and the 5-HT2A, 2C receptor agonist DOB on NMDA-evoked responses in the rat medial prefrontal cortex. *Eur J Neurosci* 11: 2917–2934, 1999.

Ayali A, Harris-Warrick RM. Monoamine control of the pacemaker kernel and cycle frequency in the lobster pyloric network. *J Neurosci* 19: 6712–6722, 1999.

Baro DJ, Levini RM, Kim MT, Willms AR, Lanning CC, Rodriguez HE, Harris-Warrick RM. Quantitative single-cell-reverse transcription-PCR demonstrates that A-current magnitude varies as a linear function of *shal* gene expression in identified stomatogastric neurons. *J Neurosci* 17: 6597–6610, 1997.

Beenhakker MP, Kirby MS, Nusbaum MP. Mechanosensory gating of proprioceptor input to modulatory projection neurons. *J Neurosci* 27: 14308–14316, 2007.

Beltz B, Eisen JS, Flamm R, Harris-Warrick RM, Hooper SL, Marder E. Serotonergic innervation and modulation of the stomatogastric ganglion of three decapod crustaceans (*Panulirus interruptus*, *Homarus americanus* and *Cancer irroratus*). *J Exp Biol* 109: 35–54, 1984.

Bidaut M. Pharmacological dissection of pyloric network of the lobster stomatogastric ganglion using picrotoxin. *J Neurophysiol* 44: 1089–1101, 1980.

Birmingham JT, Billimoria CP, DeKlotz TR, Stewart RA, Marder E. Differential and history-dependent modulation of a stretch receptor in the stomatogastric system of the crab, *Cancer borealis*. *J Neurophysiol* 90: 3608–3616, 2003.

Blitz DM, White RS, Saideman SR, Cook A, Christie AE, Nadim F, Nusbaum MP. A newly identified extrinsic input triggers a distinct gastric mill rhythm via activation of modulatory projection neurons. *J Exp Biol* 211: 1000–1011, 2008.

Bockaert J, Marin P, Dumuis A, Fagni L. The "magic tail" of G protein-coupled receptors: an anchorage for functional protein networks. *FEBS Lett* 546: 65–72, 2003.

Bucher D, Prinz AA, Marder E. Animal-to-animal variability in motor pattern production in adults and during growth. *J Neurosci* 25: 1611–1619, 2005.

Carlisle HJ, Kennedy MB. Spine architecture and synaptic plasticity. *Trends Neurosci* 28: 182–187, 2005.

Carr DB, Day M, Cantrell AR, Held J, Scheuer T, Catterall WA, Surmeier DJ. Transmitter modulation of slow, activity-dependent alterations in sodium channel availability endows neurons with a novel form of cellular plasticity. *Neuron* 39: 793–806, 2003.

Chen Y, Yu FH, Surmeier DJ, Scheuer T, Catterall WA. Neuromodulation of Na^+ channel slow inactivation via cAMP-dependent protein kinase and protein kinase C. *Neuron* 49: 409–420, 2006.

Christie AE, Stemmler EA, Peguero B, Messinger DI, Provencher HL, Scheerlinck P, Hsu YW, Guiney ME, de la Iglesia HO, Dickinson PS. Identification, physiological actions, and distribution of VYRKPPFNGSIF-amide (Val1)-SIFamide) in the stomatogastric nervous system of the American lobster *Homarus americanus*. *J Comp Neurol* 496: 406–421, 2006.

Cirelli C, Tononi G. Locus ceruleus control of state-dependent gene expression. *J Neurosci* 24: 5410–5419, 2004.

Clark MC, Baro DJ. Arthropod D2 receptors positively couple with cAMP through the Gi/o protein family. *Comp Biochem Physiol B Biochem Mol Biol* 146: 9–19, 2007.

Clark MC, Dever TE, Dever JJ, Xu P, Rehder V, Sosa MA, Baro DJ. Arthropod 5-HT2 receptors: a neurohormonal receptor in decapod crustaceans that displays agonist independent activity resulting from an evolutionary alteration to the DRY motif. *J Neurosci* 24: 3421–3435, 2004.

Colas JF, Launay JM, Kellerman O, Rosay P, Maroteaux L. *Drosophila* 5-HT2 serotonin receptor: coexpression with *fushi-tarazu* during segmentation. *Proc Natl Acad Sci USA* 92: 5441–5445, 1995.

Coleman MJ, Konstant PH, Rothman BS, Nusbaum MP. Neuropeptide degradation produces functional inactivation in the crustacean nervous system. *J Neurosci* 14: 6205–6216, 1994.

Coleman MJ, Meyrand P, Nusbaum MP. A switch between two modes of synaptic transmission mediated by presynaptic inhibition. *Nature* 378: 502–505, 1995.

Coleman MJ, Nusbaum MP. Functional consequences of compartmentalization of synaptic input. *J Neurosci* 14: 6544–6552, 1994.

Coleman MJ, Nusbaum MP, Cournil I, Claiborne BJ. Distribution of modulatory inputs to the stomatogastric ganglion of the crab, *Cancer borealis*. *J Comp Neurol* 325: 581–594, 1992.

Davis GW. Homeostatic control of neural activity: from phenomenology to molecular design. *Annu Rev Neurosci* 29: 307–323, 2006.

Di Prisco GV, Pearlstein E, Robitaille R, Dubuc R. Role of sensory-evoked NMDA plateau potentials in the initiation of locomotion. *Science* 278: 1122–1125, 1997.

Dwivedi Y, Mondal AC, Payappagoudar GV, Rizavi HS. Differential regulation of serotonin (5HT)2A receptor mRNA and protein levels after single and repeated stress in rat brain: role in learned helplessness behavior. *Neuropharmacology* 48: 204–214, 2005.

Edwards DH, Yeh SR, Musolf BE, Antonsen BL, Krasne FB. Metamodulation of the crayfish escape circuit. *Brain Behav Evol* 60: 360–369, 2002.

Fenelon VS, Le Feuvre Y, Meyrand P. Phylogenetic, ontogenetic and adult adaptive plasticity of rhythmic neural networks: a common neuromodulatory mechanism? *J Comp Physiol A Sens Neural Behav Physiol* 190: 691–705, 2004.

Flamm RE, Harris-Warrick RM. Aminergic modulation in lobster stomatogastric ganglion. I. Effects on motor pattern and activity of neurons within the pyloric circuit. *J Neurophysiol* 55: 847–865, 1986a.

Flamm RE, Harris-Warrick RM. Aminergic modulation in lobster stomatogastric ganglion. II. Target neurons of dopamine, octopamine, and serotonin within the pyloric circuit. *J Neurophysiol* 55: 866–881, 1986b.

Goaillard JM, Schulz DJ, Kilman VL, Marder E. Octopamine modulates the axons of modulatory projection neurons. *J Neurosci* 24: 7063–7073, 2004.

Golowasch J, Abbott LF, Marder E. Activity-dependent regulation of potassium currents in an identified neuron of the stomatogastric ganglion of the crab *Cancer borealis*. *J Neurosci* 19: RC33, 1999.

Harris-Warrick RM, Flamm RE. Multiple mechanisms of bursting in a conditional bursting neuron. *J Neurosci* 7: 2113–2128, 1987.

Harris-Warrick RM, Johnson BR, Peck JH, Kloppenburg P, Ayali A, Skarbinski J. Distributed effects of dopamine modulation in the crustacean pyloric network. *Ann NY Acad Sci* 860: 155–167, 1998.

Harris-Warrick RM, Marder E, Selverston AI, Moulins M. Editors. *Dynamic Biological Networks: The Stomatogastric Nervous System.* Cambridge, MA: MIT Press, 1992a.

Harris-Warrick RM, Nagy F, Nusbaum MP. Neuromodulation of stomatogastric networks by identified neurons and transmitters. In: *Dynamic Biological Networks: The Stomatogastric Nervous System*, edited by Harris-Warrick RM, Marder E, Selverston AI, Moulins M. Cambridge, MA: MIT Press, 1992b, p. 87–137.

Hooper SL, DiCaprio RA. Crustacean motor pattern generator networks. *Neurosignals* 13: 50–69, 2004.

Johnson BR, Harris-Warrick RM. Aminergic modulation of graded synaptic transmission in the lobster stomatogastric ganglion. *J Neurosci* 10: 2066–2076, 1990.

Johnson BR, Peck JH, Harris-Warrick RM. Amine modulation of electrical coupling in the pyloric network of the lobster stomatogastric ganglion. *J Comp Physiol A Sens Neural Behav Physiol* 172: 715–732, 1993.

Johnson BR, Peck JH, Harris-Warrick RM. Differential modulation of chemical and electrical components of mixed synapses in the lobster stomatogastric ganglion. *J Comp Physiol A Sens Neural Behav Physiol* 175: 233–249, 1994.

Johnson BR, Peck JH, Harris-Warrick RM. Distributed amine modulation of graded chemical transmission in the pyloric network of the lobster stomatogastric ganglion. *J Neurophysiol* 74: 437–452, 1995.

Kandel ER. The molecular biology of memory storage: a dialogue between genes and synapses. *Science* 294: 1030–1038, 2001.

Katz PS, Edwards DH. Metamodulation: the control and modulation of neuromodulation. In: *Beyond Neurotransmission: Neuromodulation and Its Importance for Information Processing*, edited by Katz PS. Oxford, UK: Oxford Univ. Press, 1999, p. 349–381.

Katz PS, Harris-Warrick RM. Neuromodulation of the crab pyloric central pattern generator by serotonergic/cholinergic proprioceptive afferents. *J Neurosci* 10: 1495–1512, 1990.

Khorkova O, Golowasch J. Neuromodulators, not activity, control coordinated expression of ionic currents. *J Neurosci* 27: 8709–8718, 2007.

Kiehn O, Harris-Warrick RM. 5-HT modulation of hyperpolarization-activated inward current and calcium-dependent outward current in a crustacean motor neuron. *J Neurophysiol* 68: 496–508, 1992.

Kirby MS, Nusbaum MP. Peptide hormone modulation of a neuronally modulated motor circuit. *J Neurophysiol* 98: 3206–3220, 2007.

Kloppenburg P, Zipfel WR, Webb WW, Harris-Warrick RM. Highly localized Ca(2+) accumulation revealed by multiphoton microscopy in an identified motoneuron and its modulation by dopamine. *J Neurosci* 20: 2523–2533, 2000.

Krenz WD, Nguyen D, Perez-Acevedo NL, Selverston AI. Group I, II, and III mGluR compounds affect rhythm generation in the gastric circuit of the crustacean stomatogastric ganglion. *J Neurophysiol* 83: 1188–1201, 2000.

Mamiya A, Nadim F. Dynamic interaction of oscillatory neurons coupled with reciprocally inhibitory synapses acts to stabilize the rhythm period. *J Neurosci* 24: 5140–5150, 2004.

Marder E, Bucher D. Central pattern generators and the control of rhythmic movements. *Curr Biol* 11: R986–R996, 2001.

Marder E, Bucher D. Understanding circuit dynamics using the stomatogastric nervous system of lobsters and crabs. *Annu Rev Physiol* 69: 291–316, 2007.

Marder E, Goaillard JM. Variability, compensation and homeostasis in neuron and network function. *Nat Rev Neurosci* 7: 563–574, 2006.

Miller JP, Selverston AI. Mechanisms underlying pattern generation in lobster stomatogastric ganglion as determined by selective inactivation of identified neurons. IV. Network properties of pyloric system. *J Neurophysiol* 48: 1416–1432, 1982.

Mitchell GS, Johnson SM. Neuroplasticity in respiratory motor control. *J Appl Physiol* 94: 358–374, 2003.

Mizrahi A, Dickinson PS, Kloppenburg P, Fenelon V, Baro DJ, Harris-Warrick RM, Meyrand P, Simmers J. Long-term maintenance of channel distribution in a central pattern generator neuron by neuromodulatory inputs revealed by decentralization in organ culture. *J Neurosci* 21: 7331–7339, 2001.

Nargeot R. Voltage-dependent switching of sensorimotor integration by a lobster central pattern generator. *J Neurosci* 23: 4803–4808, 2003.

Nebigil CG, Etienne N, Schaerlinger B, Hickel P, Launay JM, Maroteaux L. Developmentally regulated serotonin 5-HT2B receptors. *Int J Dev Neurosci* 19: 365–372, 2001.

Nowotny T, Szucs A, Levi R, Selverston AI. Models wagging the dog: are circuits constructed with disparate parameters? *Neural Comput* 19: 1985–2003, 2007.

Nusbaum MP, Beenhakker MP. A small-systems approach to motor pattern generation. *Nature* 417: 343–350, 2002.

Peck JH, Gaier E, Stevens E, Repicky S, Harris-Warrick RM. Amine modulation of I_h in a small neural network. *J Neurophysiol* 96: 2931–2940, 2006.

Peck JH, Nakanishi ST, Yaple R, Harris-Warrick RM. Amine modulation of the transient potassium current in identified cells of the lobster stomatogastric ganglion. *J Neurophysiol* 86: 2957–2965, 2001.

Perez-Acevedo NL, Krenz WD. Metabotropic glutamate receptor agonists modify the pyloric output of the crustacean stomatogastric ganglion. *Brain Res* 1062: 1–8, 2005.

Prinz AA, Bucher D, Marder E. Similar network activity from disparate circuit parameters. *Nat Neurosci* 7: 1345–1352, 2004.

Riad M, Watkins KC, Doucet E, Hamon M, Descarries L. Agonist-induced internalization of serotonin-1a receptors in the dorsal raphe nucleus (autoreceptors) but not hippocampus (heteroreceptors). *J Neurosci* 21: 8378–8386, 2001.

Rotaru DC, Lewis DA, Gonzalez-Burgos G. Dopamine D1 receptor activation regulates sodium channel-dependent EPSP amplification in rat prefrontal cortex pyramidal neurons. *J Physiol* 581: 981–1000, 2007.

Saideman SR, Blitz DM, Nusbaum MP. Convergent motor patterns from divergent circuits. *J Neurosci* 27: 6664–6674, 2007a.

Saideman SR, Ma M, Kutz-Naber KK, Cook A, Torfs P, Schoofs L, Li L, Nusbaum MP. Modulation of rhythmic motor activity by pyrokinin peptides. *J Neurophysiol* 97: 579–595, 2007b.

Saudou F, Boschert U, Amlaiky N, Plassat JL, Hen R. A family of *Drosophila* serotonin receptors with distinct intracellular signalling properties and expression patterns. *EMBO J* 11: 7–17, 1992.

Schlenstedt J, Balfanz S, Baumann A, Blenau W. Am5-HT7: molecular and pharmacological characterization of the first serotonin receptor of the honeybee (*Apis mellifera*). *J Neurochem* 98: 1985–1998, 2006.

Schulz DJ, Goaillard JM, Marder E. Variable channel expression in identified single and electrically coupled neurons in different animals. *Nat Neurosci* 9: 356–362, 2006.

Schulz DJ, Goaillard JM, Marder EE. Quantitative expression profiling of identified neurons reveals cell-specific constraints on highly variable levels of gene expression. *Proc Natl Acad Sci USA* 104: 13187–13191, 2007.

Selverston AI. A neural infrastructure for rhythmic motor patterns. *Cell Mol Neurobiol* 25: 223–244, 2005.

Selverston AI, Russell DF, Miller JP, King DG. The stomatogastric nervous system: structure and fuction of a small neural network. *Prog Neurobiol* 7: 215–290, 1976.

Sosa MA, Spitzer N, Edwards DH, Baro DJ. A crustacean serotonin receptor: cloning and distribution in the thoracic ganglia of crayfish and freshwater prawn. *J Comp Neurol* 473: 526–537, 2004.

Spitzer N, Antonsen BL, Edwards DH. Immunocytochemical mapping and quantification of expression of a putative type 1 serotonin receptor in the crayfish nervous system. *J Comp Neurol* 484: 261–282, 2005.

Spitzer N, Edwards DH, Baro DJ. Conservation of structure, signaling and pharmacology between two serotonin receptor subtypes from decapod crustaceans, Panulirus interruptus and Procambarus clarkii. *J Exp Biol* 211: 92–105, 2008.

Stein W, DeLong ND, Wood DE, Nusbaum MP. Divergent co-transmitter actions underlie motor pattern activation by a modulatory projection neuron. *Eur J Neurosci* 26: 1148–1165, 2007.

Stemmler EA, Peguero B, Bruns EA, Dickinson PS, Christie AE. Identification, physiological actions, and distribution of TPSGFLGMR-amide: a novel tachykinin-related peptide from the midgut and stomatogastric nervous system of Cancer crabs. *J Neurochem* 101: 1351–1366, 2007.

Swensen AM, Marder E. Multiple peptides converge to activate the same voltage-dependent current in a central pattern-generating circuit. *J Neurosci* 20: 6752–6759, 2000.

Szucs A, Abarbanel HD, Rabinovich MI, Selverston AI. Dopamine modulation of spike dynamics in bursting neurons. *Eur J Neurosci* 21: 763–772, 2005.

Thirumalai V, Prinz AA, Johnson CD, Marder E. Red pigment concentrating hormone strongly enhances the strength of the feedback to the pyloric rhythm oscillator but has little effect on pyloric rhythm period. *J Neurophysiol* 95: 1762–1770, 2006.

Thoby-Brisson M, Simmers J. Neuromodulatory inputs maintain expression of a lobster motor pattern-generating network in a modulation-dependent state: evidence from long-term decentralization in vitro. *J Neurosci* 18: 2212–2225, 1998.

Tierney AJ. Structure and function of invertebrate 5-HT receptors: a review. *Comp Biochem Physiol A Comp Physiol* 128: 791–804, 2001.

Turrigiano GG, Selverston AI. A cholecystokinin-like hormone activates a feeding-related neural circuit in lobster. *Nature* 344: 866–868, 1990.

Weaver AL, Hooper SL. Follower neurons in lobster (*Panulirus interruptus*) pyloric network regulate pacemaker period in complementary ways. *J Neurophysiol* 89: 1327–1338, 2003.

Witz P, Amlaiky N, Plassat JL, Maroteaux L, Borrelli E, Hen R. Cloning and characterization of a *Drosophila* serotonin receptor that activates adenylate cyclase. *Proc Natl Acad Sci USA* 87: 8940–8944, 1990.

Wohlpart KL, Molinoff PB. Regulation of levels of 5-HT2A receptor mRNA. *Ann NY Acad Sci* 861: 128–135, 1998.

Wood DE, Manor Y, Nadim F, Nusbaum MP. Intercircuit control via rhythmic regulation of projection neuron activity. *J Neurosci* 24: 7455–7463, 2004.

Wood DE, Nusbaum MP. Extracellular peptidase activity tunes motor pattern modulation. *J Neurosci* 22: 4185–4195, 2002.

Yeh S-R, Musolf BE, Edwards DH. Neuronal adaptations to changes in the social dominance status of crayfish. *J Neurosci* 17: 697–708, 1997.

Yuan LL, Chen X. Diversity of potassium channels in neuronal dendrites. *Prog Neurobiol* 78: 374–389, 2006.

Zhang B, Harris-Warrick RM. Multiple receptors mediate the modulatory effects of serotonergic neurons in a small neural network. *J Exp Biol* 190: 55–77, 1994.

Zhang B, Harris-Warrick RM. Calcium-dependent plateau potentials in a crab stomatogastric ganglion motor neuron. I. Calcium current and its modulation by serotonin. *J Neurophysiol* 74: 1929–1937, 1995.